The PIP2IT Shielding Assessment

Jean-Paul Carneiro
Fermi National Accelerator Laboratory

October 16, 2019

Abstract

The PIP-II Injector Test (PIP2IT) is a 25 MeV, H^- linac currently under installation at the CryoModule Test Facility (CMTF) at Fermilab. The accelerator serves as a R&D facility to study the feasibility of a superconducting front-end for the PIP-II linac. The shielding assessment presented in this document evaluates the PIP2IT radiation shielding of the cave enclosure to ensure that it meets the standards set forth in the Fermilab Radiological Control Manual [1].

Contents

List of Figures

1 Description of PIP2IT

Figure 1 presents a layout of PIP2IT in its final configuration. An Ion Source produces up to 15 mA, 30 keV H^- beam either in DC or pulsed mode. A Low Energy Beam Transport (LEBT) made of 3 solenoids matches the beam into a 162.5 MHz Radio-Frequency Quadrupole (RFQ) which accelerates the beam up to 2.1 MeV. A Medium Energy Beam Transport (MEBT) made of 2 doublets, 3 triplets and 3 bunching cavities matches the beam into a 162.5 MHz Half-Wave Resonator (HWR) Superconducting (SC) cryomodule. At the exit of the HWR SC cryomodule the beam reaches an energy of 10 MeV and is further accelerated to 25 MeV by a second SC cryomodule made of Single Spoke Resonators (SSR) operating at 325 MHz. As depicted in Figure 1, two pairs of horizontal and vertical slits are expected to be installed at the exit of the SSR cryomodule, in the High Energy Beam Transport (HEBT) line. The purpose of these slits is phase space reconstruction: the beam is sampled by the first slit and each beamlet consisting of about 10% of the inital beam is sampled by the second slit. An insertable Faraday Cup (FC) will collect the remaining beam leaving the second slit which is estimated to be about 1% of the initial beam. The overall length of the PIP2IT is in the order of 34 m with a beam absorber installed about 6 m downstream of the SSR cryomodule. Figure 2 shows the kinetic energy as a function of position along the injector.

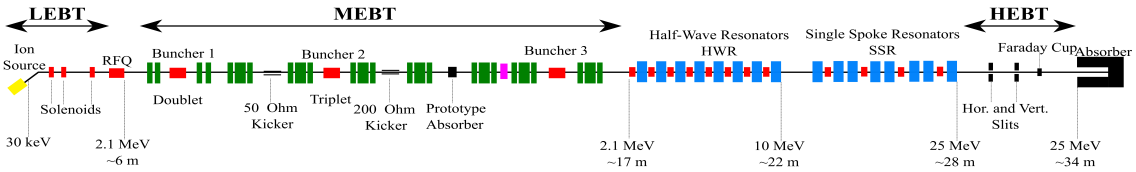

Figure 1: Layout of PIP2IT.

The injector is expected to operate at a beam average intensity of 2 mA, with a repetition rate of 20 Hz and pulse length of 0.55 msec; this corresponds to a beam power of 550 W and $1.375 \cdot 10^{14}$ H^- per second. During typical operation of the injector, the ion source will be operating at a beam current of 5 mA, either in DC mode or with long pulses (usually on the order of a few ms) and at high repetition rate (usually 60 Hz). A beam chopper located between the second and third solenoid in the LEBT, cuts pulses of 0.55 ms of beam at a repetition rate of 20 Hz. An additional bunch by bunch selection is performed in the MEBT by two 200-ohm kickers that decreases the average current in the 0.55 ms pulse from 5 mA down to 2 mA. The kicked beam is intercepted by the kicker absorber located downstream of the second kicker. The final pulse structure (0.55 ms, 20 Hz, 2 mA) is achieved at the end of the MEBT and is then injected into the HWR and SSR cryomodules

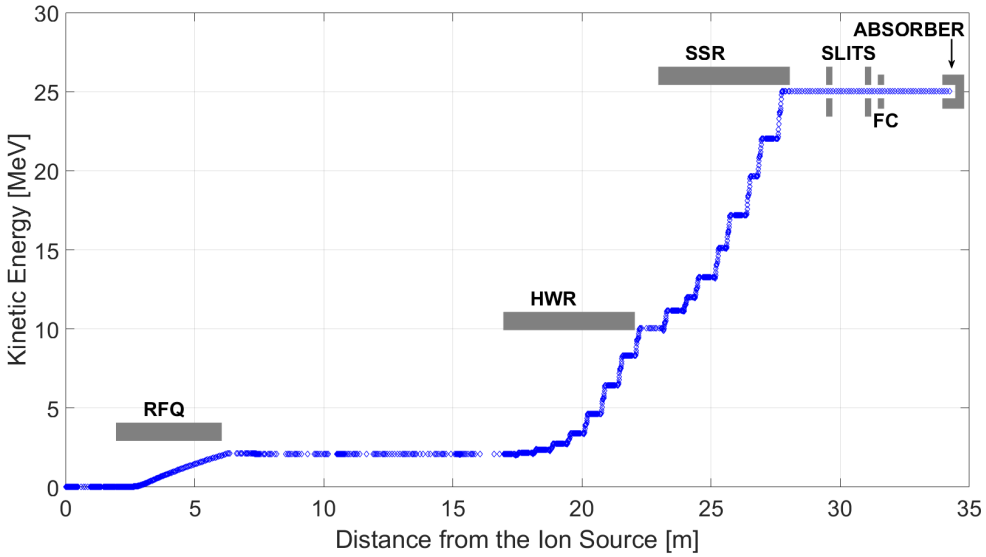

Figure 2: Kinetic energy as a function of position along PIP2IT.

to reach an energy of 25 MeV. Under normal operation, the beam is sent to a water-cooled, conical nickel-absorber at the end of the beamline.

2 Assessment Boundaries

Figure 3 shows the PIP2IT cave enclosure. The zero reference is taken as the start of the conical absorber. The North side of the cave is located about 128 ft upstream of the absorber and the South side of the cave at about 14.7 ft downstream. The East side of the cave is located at 6 ft from the beam path and the West side at 9 ft. The beam path is located at 1.3 m (about 4.3 ft) from the floor and the cave height is 10.5 ft. This document analyzes the PIP2IT cave dose rates and radiation shielding, primarily focusing on 7 areas: **The South Emergency Exit Labyrinth**, located downstream of the absorber, **the South-East Cryo Penetration**, whose entrance is located near of the exit of the HWR cryomodule, **the Four Cryo Penetrations** located in the MEBT region, **the Penetration Blocks Section**, which consists of two rows of shielding blocks containing 28 circular penetrations located on the East and West walls of the Low Energy section of the enclosure, the **North Low Energy Labyrinth**, **the Walls** and **the Roof**. Figure 4 shows the locations of these penetrations.

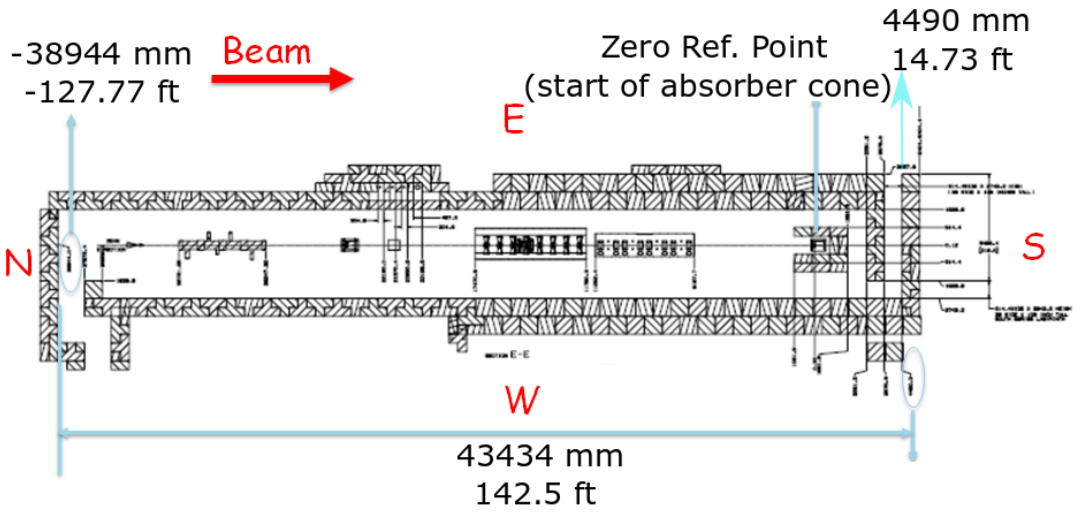

Figure 3: PIP2IT enclosure at beam level (1.3 m from the floor)

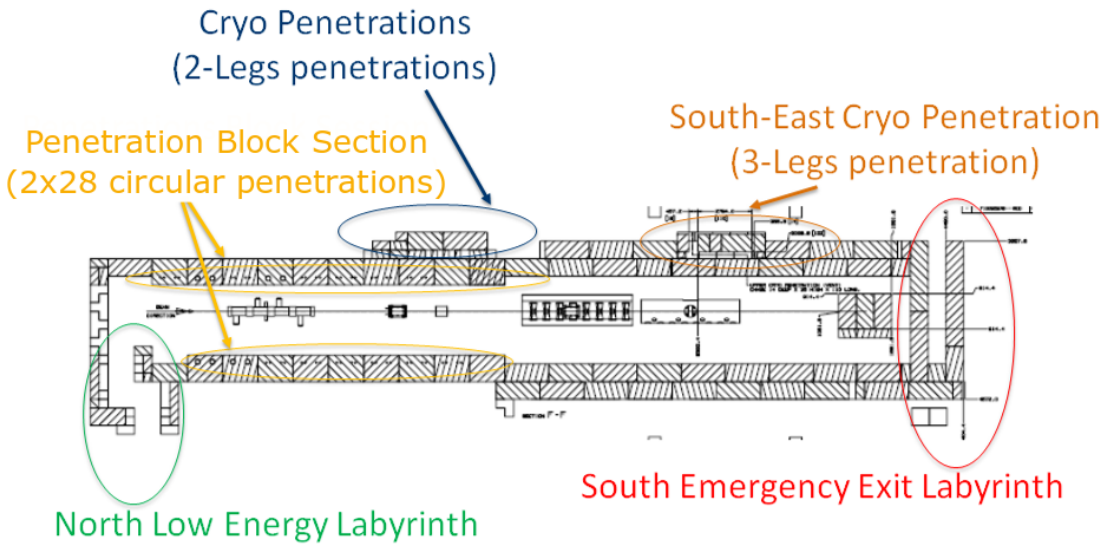

Figure 4: Plan view of PIP2IT enclosure showing the locations of the various penetrations

3 Definition of Normal and Accident Conditions

The CMTF building which hosts the PIP2IT enclosure is a Controlled Area. The area 3 ft on either side of the South Emergency Exit Labyrinth gate is assumed to be minimally occupied space. Table 1, which is based on Tables 2-6 and 2-7 in the FRCM [1], indicates the dose limits at different locations around the cave enclosure and outside the CMTF building and for two operating conditions: normal and accidental. Under normal operation, the beam is transported to the absorber or to the first slit without losses along the beamline. Most of the radiation generated under normal operation is produced at the absorber or at the first slit. Under the accident condition, the beam is entirely lost anywhere along the beamline. An interlocked detector will turn off the injector when it reaches its trip point.

The running conditions are:

1. nominal running to the absorber at 550 W (1.375×10^{14} H^-/s)
2. nominal running with losses on slits and Faraday Cup at 10 W
3. accident of losing all the 1.375×10^{14} H^- anywhere along the beamline

Area	Control Type	Normal Operating Dose Rate (mrem/hr)	Maximum Accident Dose in 1 hour (mrem)
Roof of Enclosure	Minimal Occupancy Controlled Area	0.25 to 5	< 10
Outside Enclosure (above 10.5 ft and 3 ft on either side of the South EE Labyrinth gate)	Minimal Occupancy Controlled Area	0.25 to 5	< 10
Outside Enclosure (at floor level)	Unlimited Occupancy Controlled Area	< 0.25	< 5
Outside CMTF Building	No precautions needed	< 0.05	< 1

Table 1: Allowed radiation dose rate limits in different areas as described in Table 2-6 and Table 2-7 in the FRCM.

According to Table 1, the radiation dose outside the enclosure at floor level is expected to stay below 0.25 mrem/hr under normal operation and below 5 mrem during an accident,

except 3 ft on each side of the South Emergency Exit Labyrinth gate. On the roof of the enclosure, outside the enclosure above 10.5 ft and 3 ft on each side of the South Emergency Exit Labyrinth gate, the maximum allowed dose is 5 mrem/hr during normal operation and below 10 mrem during an accident. Outside the CMTF building the maximum dose allowed is 0.05 mrem/hr during normal operation and below 1 mrem/hr during an accident.

4 Radiation Attenuation at the Absorber

The water-cooled, conical nickel-absorber was designed at Los Alamos for the Spallation Neutron Source (Oak Ridge, Tennessee) and can handle a maximum power of 20 kW. As discussed in Section 1, the injector is expected to operate at a maximum power of 550 W ($1.375 \cdot 10^{14}$ H^- per second at 25 MeV). Therefore, a large safety margin is provided by this absorber. As shown in Figure 5, the absorber is mounted inside a steel box with 1 in thick walls. The box is surrounded with 3 ft concrete blocks on the top, bottom, back and right (looking from the beam direction). On the left side of the absorber box (which is the East side of the absorber), space constraints limit the concrete shielding to 1.5 ft. The inside walls of the concrete absorber housing are expected to be entirely covered by 2 in thick steel. Also, the area surrounding the entrance of the beam tube at the absorber is expected to be shielded by bricks of steel and concrete, along with larger concrete blocks (1 ft wide, 3 ft high and 3 ft length). An estimate of the radiation attenuation through steel mentions a factor of 0.4 for 1 in of steel and a factor of 0.2 for 2 in of steel. As presented in Section 5.1, the MARS model of the absorber contains all the details of the absorber as depicted in Figure 5 (in particular the 1 in thick steel walls box around the absorber cone and the 2 in thick steel in the inside walls of the concrete absorber housing). In other words, the MARS model of the absorber represents the absorder in its final installation configuration. Concerning the dose estimates reported in this document using Equations 1 to 9 we consider only 1 in thick steel in the inside walls of the concrete absorber housing (and not 2 in thick steel in the inside walls as indicated in Figure 5) and we do not consider the 1 in thick steel walls box around the absorber cone. In other words, the dose estimates reported in this document using Equations 1 to 9 consider only 1 in steel attenuation while in its final installation configuration the absorber cone will be surrounded by 3 in steel (1 in thick steel walls box around the absorber cone and 2 in thick steel in the inside walls of the concrete absorber housing). We considered only 1 in steel attenuation for the dose estimates reported in this document using Equations 1 to 9 in order to stay conservative.

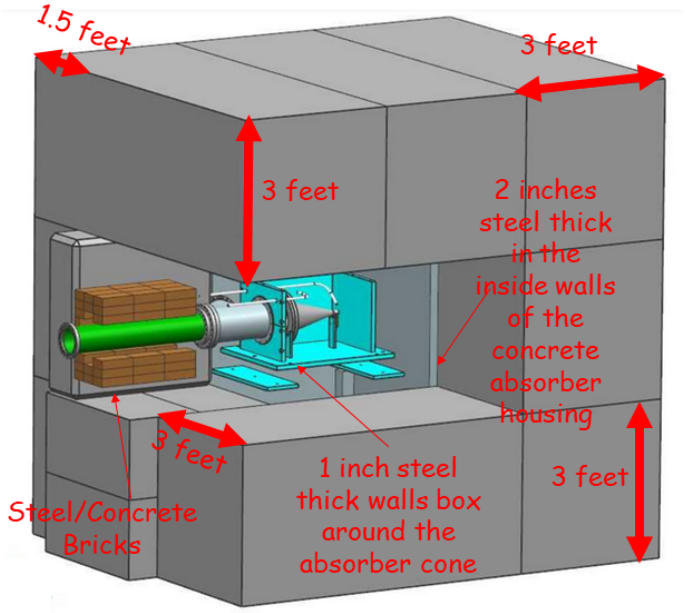

Figure 5: Shielding of PIP2IT absorber.

5 MARS Model and Simulations on the Fermi Grid

5.1 MARS Model: Absorber and Slit

A model of the absorber and the South Exit Labyrinth has been implemented into MARS [7] as shown in Figures 6(a) and 6(b). As indicated on Figures 6(a) and 6(b), a 2 in thick layer of steel has been implemented on the inside (east, west, downstream and top) of the concrete blocks surrounding the absorber. This steel is expected to be installed before the start of the operation of the accelerator. This layer is simulated as regular steel in MARS. The water-cooled, conical nickel-absorber is confined inside a box of 1 in thick steel which is also modeled in MARS. Figures 7(a) and 7(b) show a layout of the PIP2IT beam absorber inside its 1 in steel box and surrounded by the concrete blocks. Steel bricks will be placed at the entrance of the absorber and this shielding is implemented in the MARS model as regular steel. As presented in Section 15, two pairs of slits are expected to be installed in the HEBT line for horizontal and vertical phase space reconstruction. The slit is implemented in MARS as a TMZ plates of 20 mm high, 20 mm wide and 2 mm thick in the beam direction, located 4337.6 mm from the absorber cone entrance, as indicated in Figures 6(a) and 6(b).

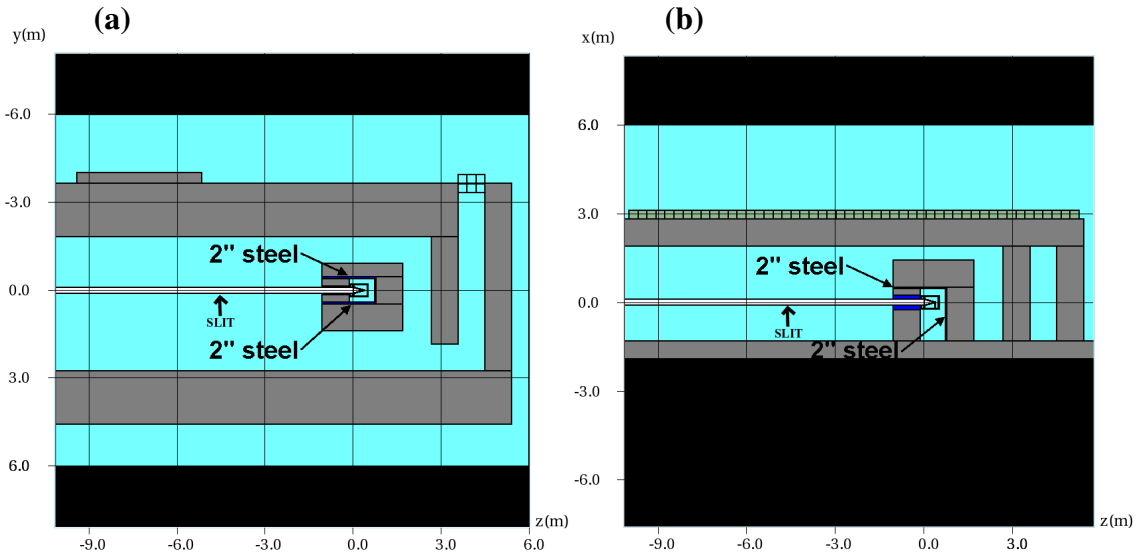

Figure 6: MARS Model of the PIP2IT Absorber and South Exit Labyrinth (a) plan view and (b) side view.

5.2 MARS on Fermi Grid: Simulations performed and Error rates

Two sets of MARS simulations have been performed on the Fermi Grid [2] using the model shown in Figures 6(a) and 6(b): the absorber has been simulated with 4000 runs and the slit with 2000 runs. Each set of simulations have been performed with $1.5E7$ particles per run for 550 W (at the absorber or at Slit1). For the simulation concerning the absorber and presented in Sections 7, 8, 12 and 14 the error rates on the MARS results for the various penetrations of interest (South Emergency Exit Labyrinth, South-East Cryo Penetration, Roof and Residual Dose) ranged from less than 10% to nearly 100%. However, given the general agreement presented in Table 6 and Table 7 between the calculated results and the MARS results, additional MARS runs to reduce the larger errors were deemed unnecessary. For the slit MARS simulations, any region of interest in the MARS model had errors below 10%, except for the South-East Cryo Penetration presented in Section 15.5, whose regions of interest had errors between 20% and 42%.

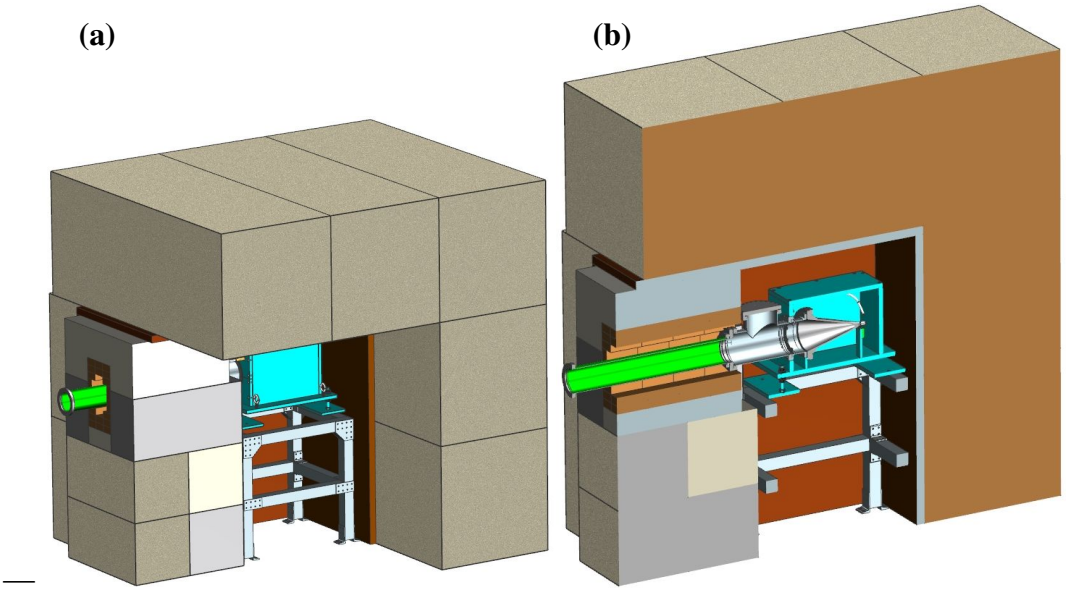

Figure 7: Layout of the PIP2IT beam absorber inside its 1 in steel box and surrounded by the concrete blocks.

6 Assessment Methodology

Based on information from Sullivan [3], K. Vaziri derived Equation 1 which determines the radiation dose in mrem as a function of energy E measured in units of GeV, distance r in ft, and angle θ_s (Sullivan Angle in deg) from a low energy proton (< 1 GeV) incident upon a target:

$$S(E, r, \theta_s) = \frac{2 \cdot 10^{-5}(1 + E^{0.6})(1 - e^{-3.6E^{1.6}})}{\left(0.3r\left(\theta_s + \frac{40}{\sqrt{E}}\right)\right)^2} \tag{1}$$

Based on Equation 2.17 of Ref. [4], the neutron fluence Θ at 1 m and at an angle θ_s to the direction of an incident proton below 1 GeV of energy E in GeV is given by:

$$\Theta\left(\frac{neutrons}{m^2}\right) = \frac{5000 \times (1 - e^{-m})}{\left(\theta_s + \frac{40}{\sqrt{E}}\right)^2} \quad \text{with} \quad m = 3.6 \times E^{1.6} \tag{2}$$

Equation 3 is based on Equation 1.29 in Ref. [4] and gives the conversion factor C_H from

neutron fluence to dose, the neutron fluence in units of neutrons/m^2 and the dose in units of fSv. The dose is considered at a depth of 1 cm in tissue-equivalent material.

$$C_H = 40(1 + E^{0.6}) \quad \text{fSv per neutrons} \cdot m^{-2} \tag{3}$$

The fluence Θ to dose S conversion at a distance r in meters is given by the equation:

$$S(E, r, \theta_s) = \Theta\left(\frac{\text{neutrons}}{m^2}\right) \times \left(\frac{\text{conversion of neutrons}}{m^2}\text{to dose}\right) \times \frac{1}{r(m)^2} \tag{4}$$

Implementing Equations 2 and 3 into 4 and considering that 1 fSv=10^{-10} mrem and that 1 ft=0.30 m leads to Equation 1.

A Geometric Correction Factor is necessary to adjust the source term at the entrance of labyrinths and penetrations. This correction factor is shown in Equation 5 in the case of an aperture perpendicular to the direction of the beam (Figure 8(a)):

$$f(R, D) = \frac{R}{\sqrt{R^2 + D^2}} \tag{5}$$

and in Equation 6 in the case of an aperture in the same direction as the beam (Figure 8(b)):

$$f(R, D) = \frac{D}{\sqrt{R^2 + D^2}} \tag{6}$$

As shown in Figures 8, the distance D is the longitudinal distance along the beamline between the loss point and the center of the aperture. The distance R is the transverse distance between the center of the aperture and the beamline. Figure 9 illustrates the values of R in the case where the center of the aperture is located at the same height as the beam line (Fig. 9(a)) and at a different height than the beamline (Fig. 9(b)).

For labyrinths, Cossairt [5] reports that H_1 (δ_1) is the dose rate at a distance δ_1 in the first leg as measured from the mouth of the passageway in "units" of the square root of the cross-sectional area of the first leg, where H_0(R) is the dose at the mouth:

$$H_1\left(\delta_1\right) = \left[\frac{r_0}{\delta_1 + r_0}\right]^2 \times H_0(R) \quad \text{with} \quad r_0 = 1.4 \tag{7}$$

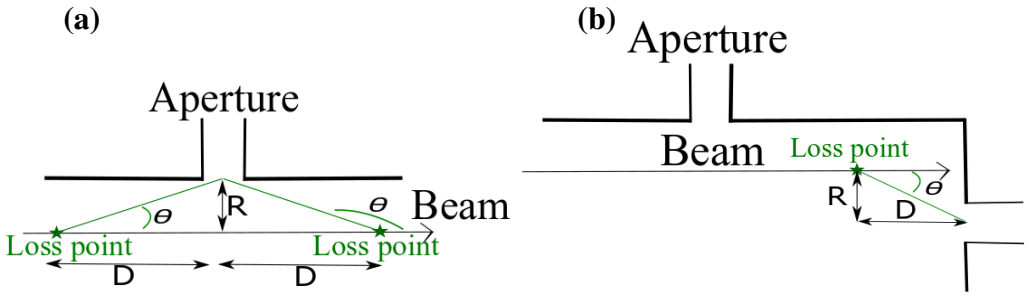

Figure 8: Definition of the R and D distances used in labyrinth and penetration calculations in the case of an aperture (a) Perpendicular to the beam direction and (b) In the beam direction.

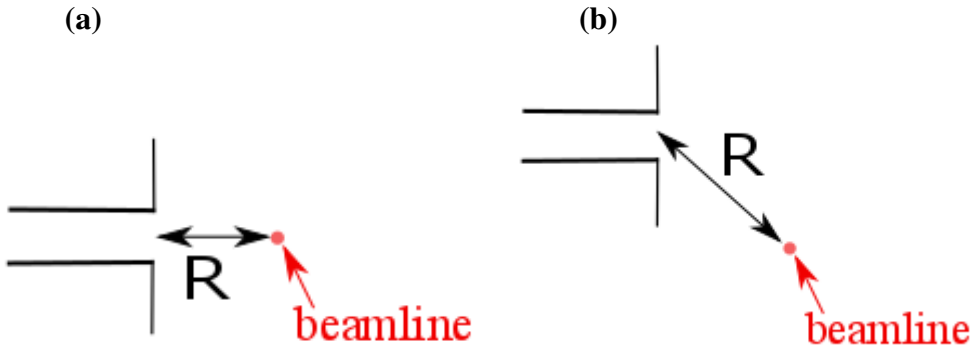

Figure 9: Definition of the distance R for an aperture located (a) at the beam height and (b) higher than the beam height

For second and successive legs of labyrinths, Cossairt [5] reports the following expression for the dose rate at a distance δ_i in the i^{th} leg measured in "units" of the square root of the cross-section area of the i^{th} leg ($i > 1$):

$$H_i(\delta_i) = \left[\frac{exp\left(-\frac{\delta_i}{a}\right) + A \times exp\left(-\frac{\delta_i}{b}\right) + B \times exp\left(-\frac{\delta_i}{c}\right)}{1 + A + B}\right] \times H_{i-1}\left(\delta_{i-1}\right) \qquad (8)$$

$$(with: a = 0.17, b = 1.17, c = 5.25, A = 0.21, B = 0.00147)$$

The radiation attenuation provided by T_{conc} feet of concrete is given by the following expression with E the neutron energy in GeV [6]:

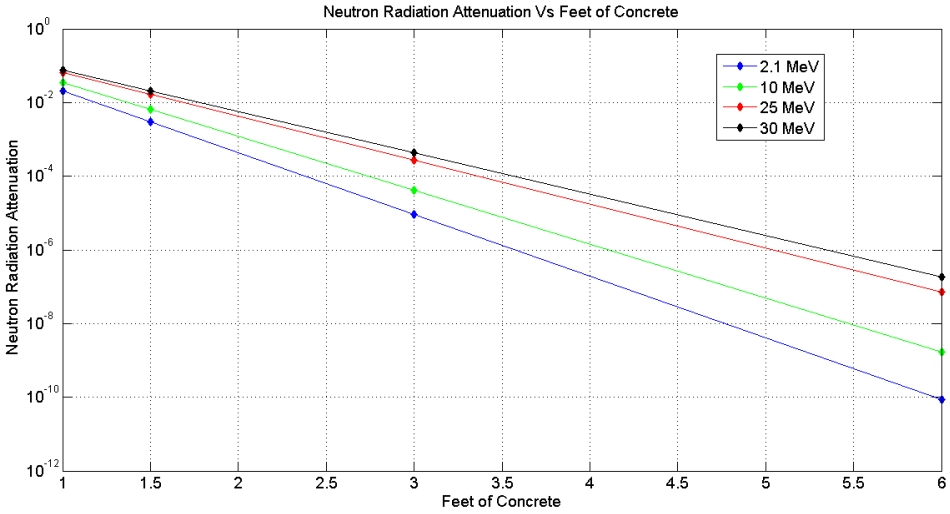

Figure 10: Neutron Radiation Attenuation Vs Feet of Concrete. From Equation 9.

$$A(E) = 10^{\frac{-T_{conc}}{2.86}/(1-0.8exp(-5\times E))} \tag{9}$$

For 25 MeV neutrons, Equation 9 predicts an attenuation of $1.6 \cdot 10^{-2}$, $2.7 \cdot 10^{-4}$ and $7.3 \cdot 10^{-8}$ respectively for 1.5 ft, 3 ft and 6 ft of concrete. Figure 10 shows attenuation factors for different concrete lengths and beam energies.

7 South Emergency Exit Labyrinth

The South Emergency Exit Labyrinth is shown in Figure 11. Leg-1 is 7.5 ft high and Leg-2 is 9 ft high. For simplicity and to keep conservative, we consider the height of Leg-1 and Leg-2 to be the same at 9 ft.

7.1 Dose rate at the exit of the 2-Legs South Emergency Exit Labyrinth during normal operation

The following parameters can be deduced from Figure 11 concerning the South Emergency Exit Labyrinth: $R = 7.5$ ft, $D = 8.73$ ft, $r = 11.50$ ft, $\theta_s = 40.6°$ and E=0.025 GeV.

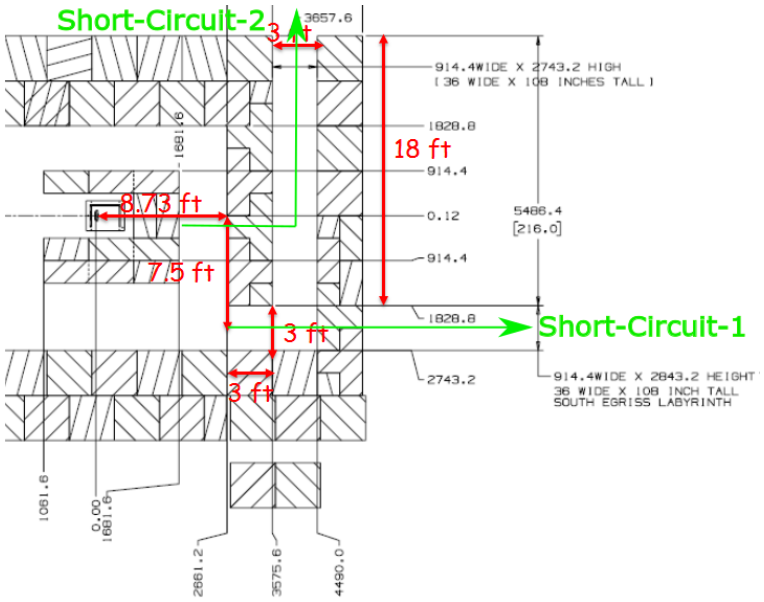

Figure 11: Drawing of the South Emergency Exit Labyrinth.

Taking the above parameters and $1.375 \cdot 10^{14}$ H^- at 25 MeV, Equation 1 reports that the dose at the entrance of Leg-1 is $7.7 \cdot 10^4$ mrem/hr considering the Geometric Correction Factor given in Equation 6 and considering no shielding (no concrete nor steel) around the absorber. Concerning Leg-1, its width is 3 ft, its height 9 ft and its length 4.5 ft. The cross-sectional area of Leg-1 is $A_1 = 27$ ft^2. According to Equation 7, $\delta_1 = 4.5/(\sqrt{27}) = 0.86$ and the attenuation factor through Leg-1 of the south labyrinth is $[1.4/(0.86 + 1.4)]^2 = 0.38$. The width of Leg-2 is 3 ft, the high 9 ft and the length 19.5 ft. The cross-sectional area of Leg-2 is $A_2 = 27$ ft^2. According to Equation 8, $\delta_2 = 19.5/(\sqrt{27}) = 3.75$ and the attenuation factor through Leg-2 is $7.6 \cdot 10^{-3}$. Therefore, the dose at the exit of the South Emergency Exit labyrinth without any attenuation around the absorber is given by the dose at the labyrinth entrance times the attenuation of Leg-1 and Leg-2 which equals: $7.7 \cdot 10^4 \times 0.38 \times 7.6 \cdot 10^{-3} = 222$ mrem/hr. If we consider 1 in of steel and 3 ft of concrete shielding around the absorber, the dose at the exit of the labyrinth is now given by 222 mrem/hr $\times$ $2.7 \cdot 10^{-4} \times 0.4 = 2.4 \cdot 10^{-2}$ mrem/hr, which is about 10 times lower than the required 0.25 mrem/hr reported in Table 1. Considering the most conservative case of 1.5 ft of concrete shielding around the absorber and 1 in of steel the dose at the exit of the labyrinth is 222 mrem/hr $\times$ $1.6 \cdot 10^{-2} \times 0.4 = 1.4$ mrem/hr which is about $1/3$ the Table 1 limit.

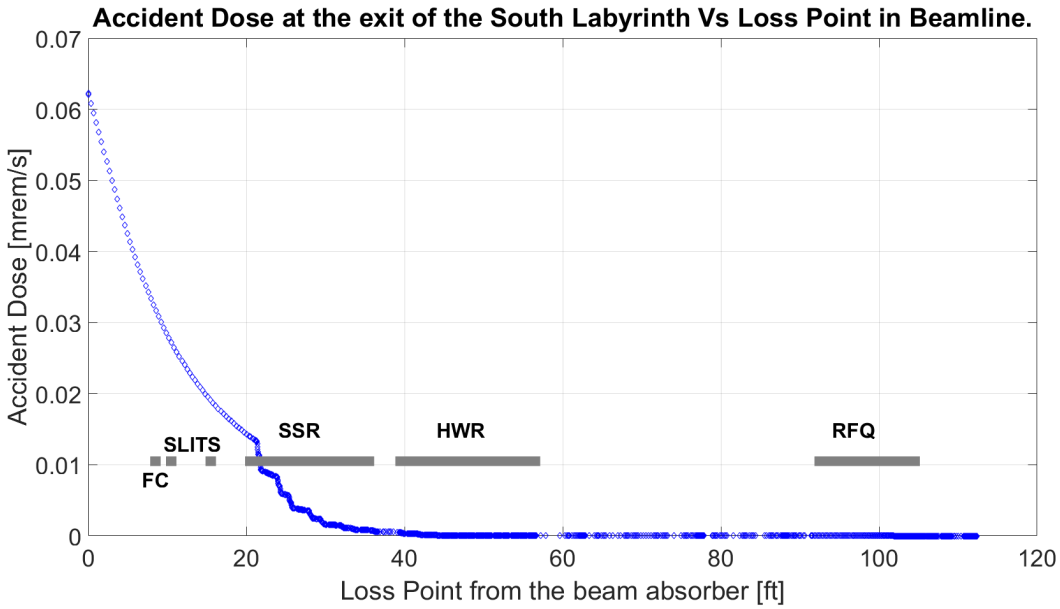

Figure 12: Accident dose at the exit of the South Emergency Exit Labyrinth as a function of the beam loss along the beamline.

7.2 Dose rate at the exit of the 2-Legs South Emergency Exit labyrinth after an accident

Figure 12 shows the expected accident dose at the exit of the labyrinth calculated using Equations 1-9 and the energy along the injector presented in Figure 2. It is presented in Figure 12 that the expected maximum accident dose rate at the South Emergency-Exit Labyrinth gate is about 6.2×10^{-2} mrem/s for a beam loss occuring just before the aborber. A beam loss occuring about 28.25 ft upstream the absorber (about half-way inside the SSR cryomodule) is expected to generate a dose at the South Emergency-Exit Labyrinth gate of about 2.8×10^{-3} mrem/s (corresponding to about 10 mrem in 1 hour) and a beam loss occuring at about 32 ft upstream the absorber is expected to generate a dose at the gate of about 1.4×10^{-3} mrem/s (corresponding to about 5 mrem in 1 hour). A beam loss at the start of the SSR cryomodule located about 36 ft from the absorber and where the beam energy is 10 MeV will generate a dose at the gate of about 7.6×10^{-4} mrem/s.

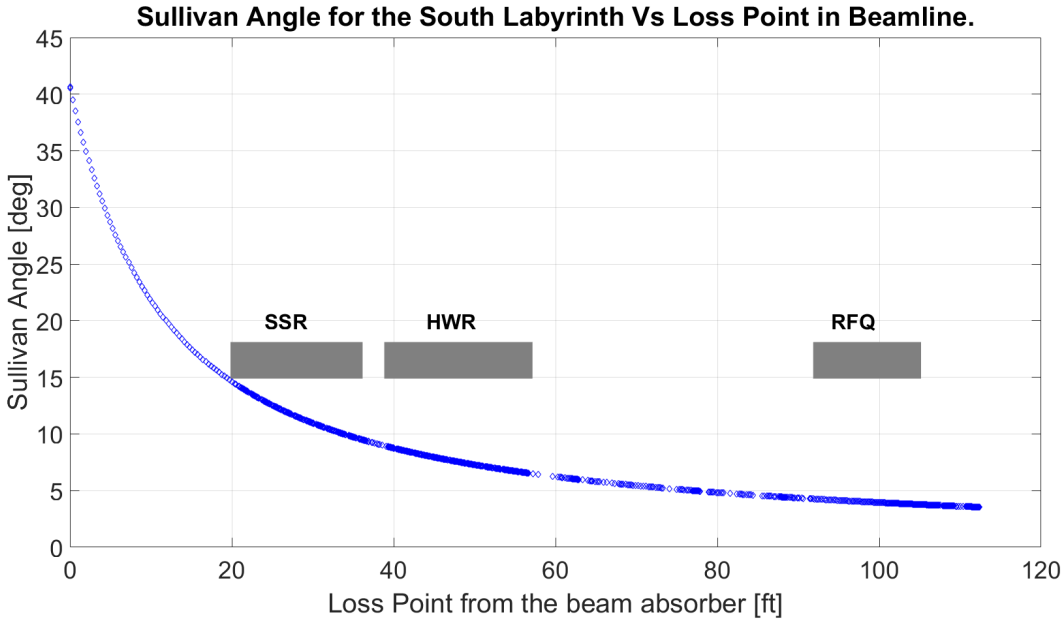

Figure 13: Sullivan Angle for the South Emergency Exit Labyrinth as a function of the position of the beam loss along the beamline.

7.3 Dose rate at the exit of the South Emergency Exit Labyrinth Short-Circuits

As indicated in Figure 11, two Short-Circuits should be considered for the South Emergency Exit Labyrinth. The first one (noted Short-Circuit-1 in Figure 11) allows the radiation from Leg-1 to reach the outside of the enclosure through the 3 ft South Wall. As discussed in Section 7.1 the dose at the entrance of Leg-1 of the labyrinth is $7.7 \cdot 10^4$ mrem/hr considering the Geometric Correction Factor given in Equation 6 and considering no shielding (no concrete nor steel) around the absorber. Attenuation through Leg-1 is about 0.38. The 3 ft South Wall brings another $2.7 \cdot 10^{-4}$ attenuation. Therefore, the dose at the exit of the 3 ft wall can be estimated at $7.7 \cdot 10^4 \times 0.38 \times 2.7 \cdot 10^{-4} = 8$ mrem/hr without consideration of shielding at the absorber. If we consider 1 in thick steel and 1.5 ft concrete the dose will then be reduced to $8 \times 6.4 \cdot 10^{-3} = 5.1 \cdot 10^{-2}$ mrem/hr which is about 5 times lower than the 0.25 mrem/hr limit. Noteworthy is the fact that the part of the absorber facing Leg-1 has 3 ft thick walls and therefore the 1.5 ft absorber shielding is conservative. A 1 in thick steel and 3 ft thick concrete at the absorber brings the dose down to $8 \times 1.1 \cdot 10^{-4} = 8.8 \cdot 10^{-4}$ mrem/hr which is about 300 times lower than the

0.25 mrem/hr limit. In the case of a beam accident, the maximum dose at the entrance of Leg-1 can be estimated at about 21 mrem/s making the dose at the exit of the South Wall at about $2.2 \cdot 10^{-3}$ mrem/s.

The second short-circuit (noted Short-Circuit-2 in Figure 11) allows radiation to reach the outside gate of the South Emergency Exit Labyrinth through the 3 ft wall located just behind the absorber and through 12 ft of the Labyrinth leg. Equation 1 estimates the radiation from the absorber on the inside part of the 3-ft wall to be about $2.4 \cdot 10^5$ mrem/hr without consideration of shielding from the absorber. If we consider an absorber with 1 in thick steel and 1.5 ft concrete this dose will be reduced to $2.4 \cdot 10^5 \times 6.4 \cdot 10^{-3} = 1536$ mrem/hr. Considering the 3 ft wall brings $2.7 \cdot 10^{-4}$ attenuation factor and the 12 ft leg give another 0.1 attenuation factor, the estimated dose rate at the South Emergency Exit Labyrinth gate through the Short-Circuit-2 is estimate to be $1536 \times 2.7 \cdot 10^{-4} \times 0.1 = 0.04$ mrem/hr, which is about 6 times lower than the 0.25 mrem/hr limit. In the case of a beam accident, the maximum dose on the inside part of the 3-ft wall behind the absorber is estimated at 67 mrem/s which is reduced to $67 \times 2.7 \cdot 10^{-4} \times 0.1 = 1.8 \times 10^{-3}$ mrem/s after being attenuated by the 3 ft wall and the 12 ft leg.

7.4 MARS Dose rate at the exit of the South Emergency Exit Labyrinth including Short-Circuits

Figure 14 shows a plan view at beam height of MARS simulation of the total effective dose from the absorber at 550 W of beam power. Figure 15 shows a detailed total effective dose at the South Emergency Exit Labyrinth with a max dose of 1.1 mrem/hr. This dose is of the same order as the one calculated analytically at 1.4 mrem/hr (for 1.5 ft of concrete around the absorber and 1 in of steel) and presented in Section 7.1.

8 South-East Cryo Penetration

Figure 16 shows the South-East Cryo Penetration. The entrance and exit of the penetration are 1.5 ft wide, 1.5 ft tall and 3 ft long. The height of the entrance penetration is located between 2743.2 mm and 3200.4 mm. The cryo chase is 1.16 ft wide and 3 ft high. The exit penetration is located at a lower height than the entrance penetration. The exit penetration is located between 2260.6 mm and 2743.2 mm. For simplicity and to keep conservative, we consider the exit penetration to be at the same height as the entrance one.

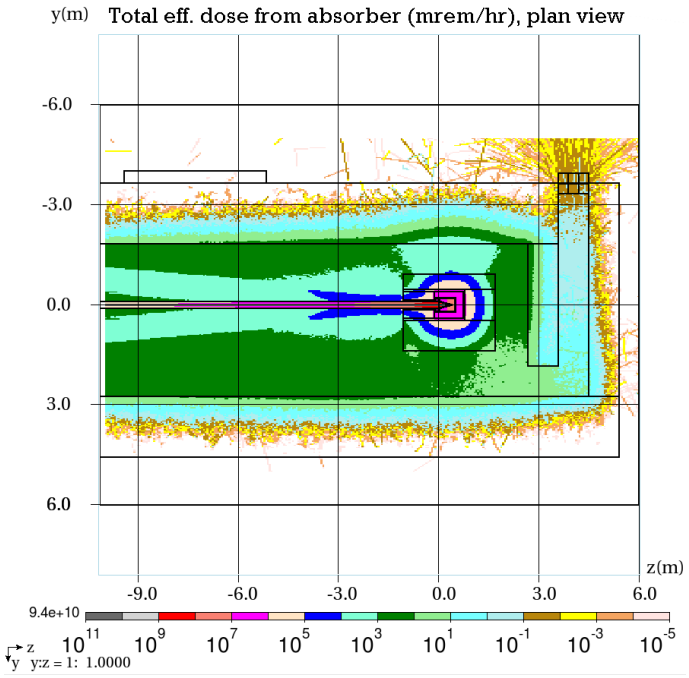

Figure 14: MARS Total Effective Dose from the absorber (plan view) under normal beam operation.

8.1 Dose rate at the exit of the South-East Cryo Penetration during normal operation

The following parameters can be deduced from Figure 16 concerning the South-East Cryo Penetration with radiation from the absorber: $R = 8.13$ ft, $D = 18.77$ ft, $r = 20.45$ ft, $\theta_s = 156.6°$ and E=0.025 GeV. Taking the above parameters and $1.375 \cdot 10^{14}$ H^- at 25 MeV, Equation 1 reports that the dose at the entrance of Leg-1 of the South-East Cryo Penetration is about $6.5 \cdot 10^3$ mrem/hr taking into account the Geometric Correction Factor correction given in Equation 5 and considering no shielding (no concrete nor steel) around the absorber. Leg-1 of the penetration has a width of 1.5 ft, a height of 1.5 ft and a length of 3.58 ft. The cross-sectional area of Leg-1 is $A_1 = 2.25$ ft^2. According to Equation 7, $\delta_1 = 3.58/(\sqrt{2.25}) = 2.38$ and the attenuation factor of Leg-1 is $[1.4/(2.38 + 1.4)]^2 = 0.13$.

The width of Leg-2 is 1.16 ft, the height 3 ft and the length 10.67 ft. The cross-sectional area of the second leg is $A_2 = 3.5$ ft^2. According to Equation 8, $\delta_2 = 10.67/(\sqrt{3.5}) = 5.7$

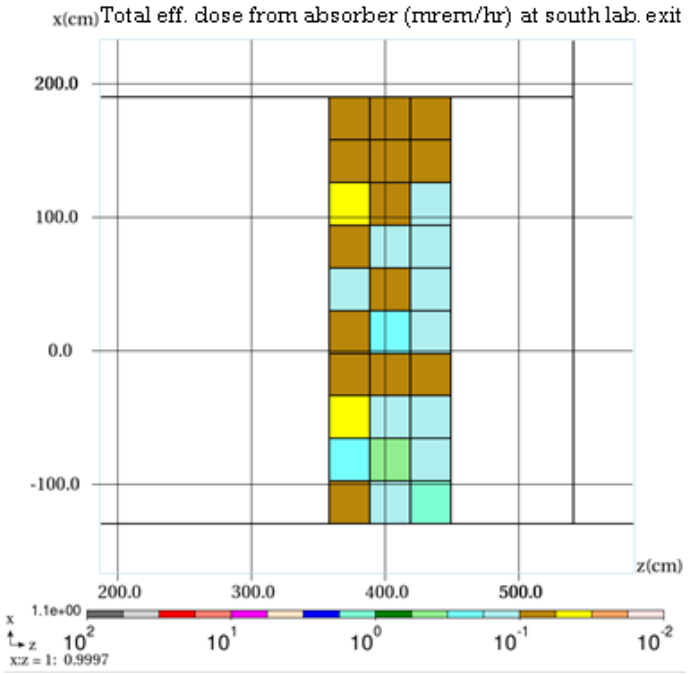

Figure 15: MARS Total Effective Dose Rate from the absorber at the South Emergency Exit Labyrinth gate under normal beam operation

and the attenuation factor through Leg-2 is $1.7 \cdot 10^{-3}$. The width of Leg-3 is 1.5 ft, the height 1.5 ft and the length 3.58 ft. The cross-sectional area of the third leg is $A_3 = 2.25$ ft^2. According to Equation 8, $\delta_3 = 3.58/(\sqrt{2.25}) = 2.38$ and the attenuation factor through Leg-3 is $23.3 \cdot 10^{-3}$. Therefore, the expected dose rate at the exit of the South-East Cryo Penetration coming from the absorber under normal operation and considering a conservative 1.5 ft of concrete shielding and 1 in of steel is expected to be: $6.5 \cdot 10^{3} \times 0.13 \times 1.7 \cdot 10^{-3} \times 23.3 \cdot 10^{-3} \times 6.4 \cdot 10^{-3} = 2.1 \cdot 10^{-4}$ mrem/hr which is about 1000 times lower than the tolerated dose of 0.25 mrem/hr. The South-East Cryo Penetration is capable of attenuating the radiation from the absorber. Also, as previously mentioned the fact that the exit aperture is at a lower height than the entrance aperture will contribute another attenuation factor which was not considered.

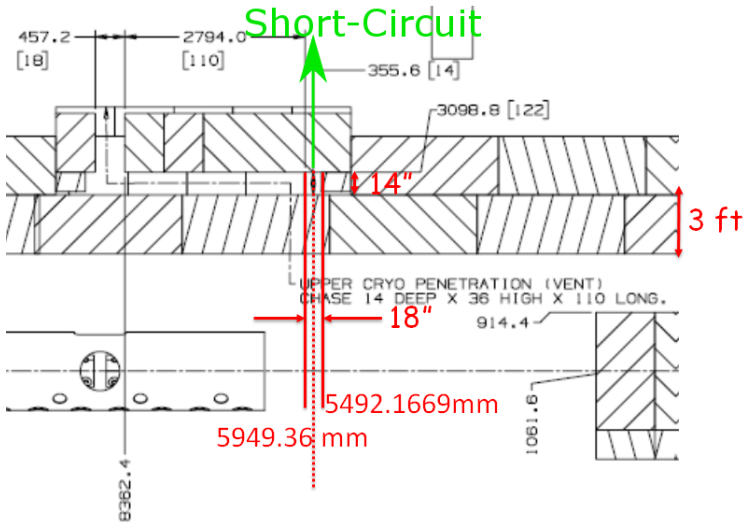

Figure 16: Drawing of the South-East Cryo Penetration.

8.2 Dose rate at the exit of the South-East Cryo Penetration during an accident

The radiation dose at the exit of the South-East Cryo Penetration during an accident is reported in Figure 17. The maximum dose in the event of a beam accident is about $2.3 \cdot 10^{-4}$ mrem/s which is significantly lower than the accident dose limit reported in Table 1. We also observe from Figure 17 that the maximum dose at the exit of the South Cryo Penetration occurs when the beam is lost about 1 ft upstream of the aperture which corresponds to the exit of the SSR cryomodule where the beam is at 25 MeV.

Figure 18 shows the Sullivan Angle computed at the South Cryo Penetration entrance for a beam loss along the beamline. At the South-East Cryo Penetration entrance the Sullivan Angle is at 90°.

8.3 Dose rate at the exit of the South-East Cryo Penetration Short-Circuits

The Short-Circuit of the South-East Cryo Penetration is shown in Figure 16. At the exit of Leg-1 radiation can reach the outside of the enclosure through a 3 ft concrete wall. The dose at the exit of the South-East Cryo Penetration Short-Circuit shown in Figure 16

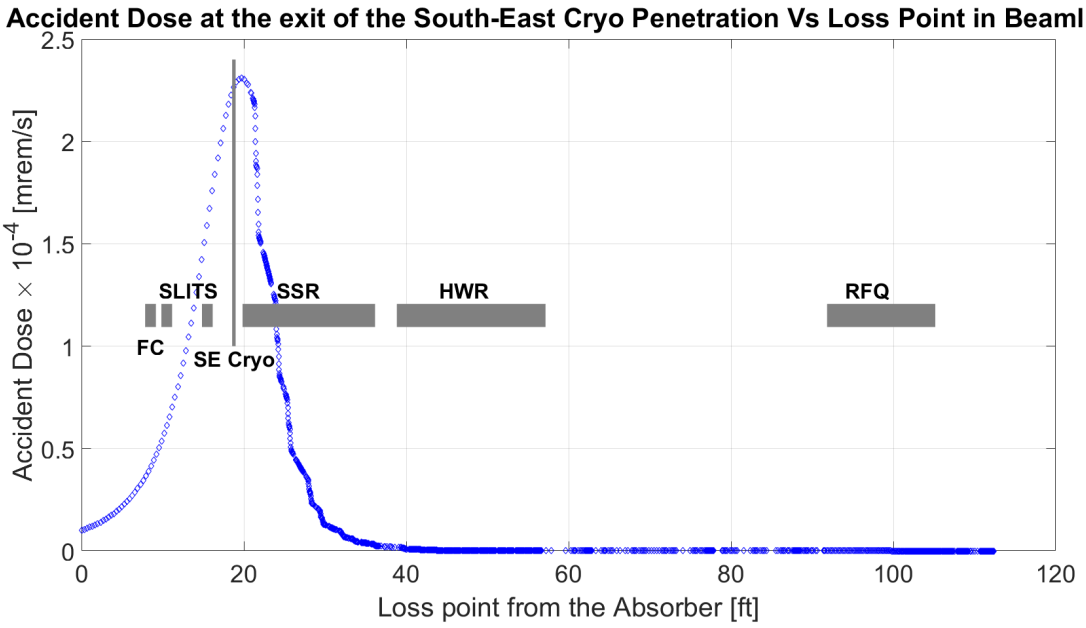

Figure 17: Accident dose at the exit of the South-East Cryo Penetration as a function of the beam loss along the beamline.

is estimated under normal operation at: $6.5 \cdot 10^3 \times 0.13 \times 2.7 \cdot 10^{-4} \times 6.4 \cdot 10^{-3} = 1.5 \cdot 10^{-3}$ mrem/hr considering the 3 ft concrete shielding for the Leg-1 exit and a 1 in steel and 1.5 ft concrete attenuation at the absorber. During an accident, the maximum dose at the entrance of the South-East Cryo Penetration is estimated to be in the order of 40 mrem/s which is attenuated to $1.4 \cdot 10^{-3}$ mrem/s after the 0.13 attenuation factor of Leg1 and 3 ft concrete at the exit of the Short-Circuit of the South-East Cryo Penetration.

8.4 MARS dose rate at the exit of the South-East Cryo Penetration including Short-Circuits

Figure 19 shows MARS Total effective dose at the South-East Cryo Penetration Exit for a beam power of 550 W at the absorber. The max dose rate predicted by MARS is $4.3 \cdot 10^{-3}$ mrem/hr, higher than the dose rate of $1.5 \cdot 10^{-3}$ mrem/hr calculated from analytics formula but still significantly lower than the tolerated dose of 0.25 mrem/hr.

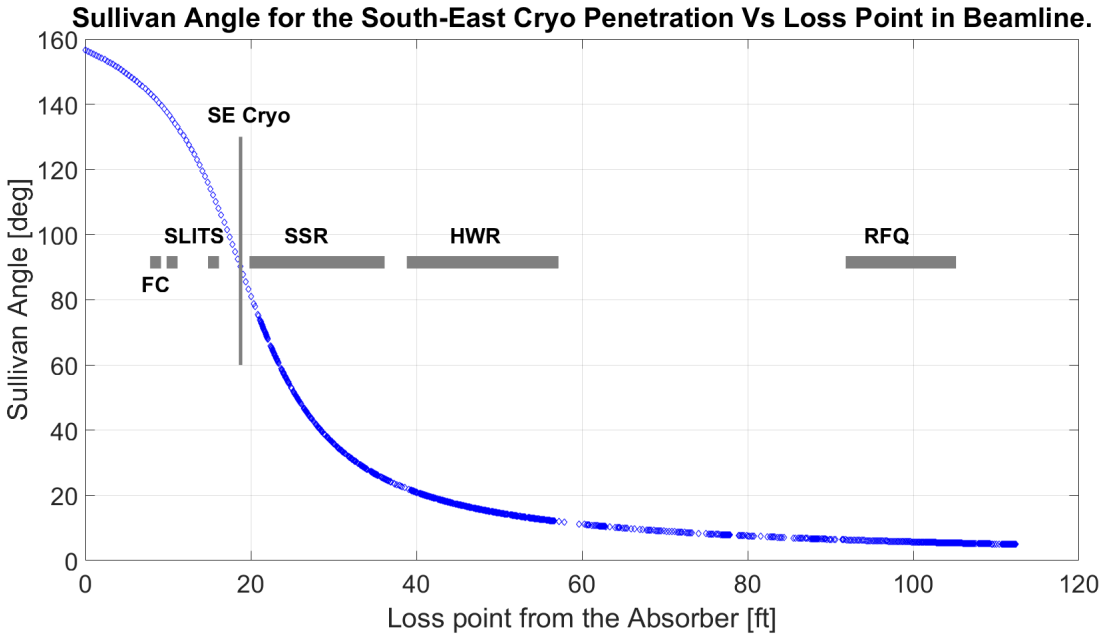

Figure 18: Sullivan Angle for the South-East Cryo Penetration as a function of the position of the beam loss along the beamline.

9 Four South-Cryo Penetrations

Figure 20 shows a drawing of the four Cryo Penetrations at floor level. The Cryo Penetrations are 2-Legs penetrations. Leg-1 at floor level are all 3 ft high and 4.5 ft length. Concerning their widths, the Leg-1 close to the absorber has a width of 1.5 ft and the three other Leg-1 have a width of 1 ft as indicated in Figure 20. Leg-2 are all 111-in long, 1.5 ft high and either 1.5 ft in width (for the Leg-2 closer to the absorber) or 1 ft in width for the 3 other Leg-2.

9.1 Dose rate at the exit of the Four South-East Cryo Penetrations during normal operation

Figure 21 shows the exit of the penetrations as seen from the top of the roof. Since the exit of the penetration are relatively close to each other (2.25 ft middle to middle), K. Vaziri suggested to consider the two Cryo Penetrations closer to the absorber as one (Cryo 1,

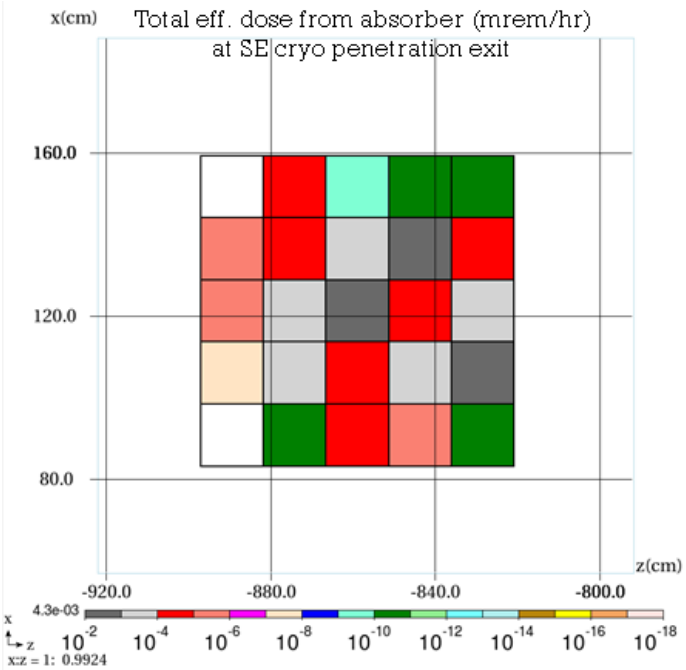

Figure 19: MARS Total Effective Dose at South-East Cryo Penetration Exit under normal operation at the absorber.

Figure 20) and the two Cryo Penetrations further away from the absorber as one (Cryo 2, Figure 20). Therefore, Leg-1 of Cryo-1 is located at 68.14 ft from the absorber, with $R = 6.58$ ft, $r = 68.46$ ft and, $\theta_s = 174.5°$ at E=0.025 GeV. The dose at the entrance of Cryo-1 from the absorber is estimated from Equation 1 to be about 130 mrem/hr, considering the Geometric Correction Factor of Equation 5 and without any shielding at the absorber. Cryo-2 is located at 72.27 ft and the dose from the absorber at the entrance of Leg-1 of Cryo-2 is estimated to be about 109 mrem/hr. Leg-1 of Cryo-1 has a width of 2.5 ft, a height of 3 ft and a length of 3.75 ft. Following Equation 7, the attenuation of Leg-1 of Cryo-1 is 0.25. Leg-1 of Cryo-2 has a width of 2 ft, a height of 3 ft and a length of 3.75 ft. The attenuation of Leg-1 of Cryo-2 is about 0.23. Leg-2 of Cryo-1 has a width of 2.5 ft, a height of 3 ft and a length of 10.75 ft. Following Equation 8, the attenuation of Leg-2 of Cryo-1 is $6.6 \cdot 10^{-3}$. Leg-2 of Cryo-2 has a width of 2 ft, a height of 3 ft and a length of 10.75 ft making an attenuation factor of $4.6 \cdot 10^{-3}$. Without any shielding at the absorber, the dose at the exit of Cryo-1 is estimated to be $130 \times 0.25 \times 6.6 \cdot 10^{-3} = 0.2$ mrem/hr and at the exit of Cryo-2 $109 \times 0.23 \times 4.6 \cdot 10^{-3} = 0.12$ mrem/hr. Considering 1 in steel and 1.5 ft concrete attenuation at the absorber, the dose at the exit of the Cryo-1 and Cryo-2 penetrations are expected to be in the order of $1 \cdot 10^{-3}$ mrem/hr, about 250 times lower

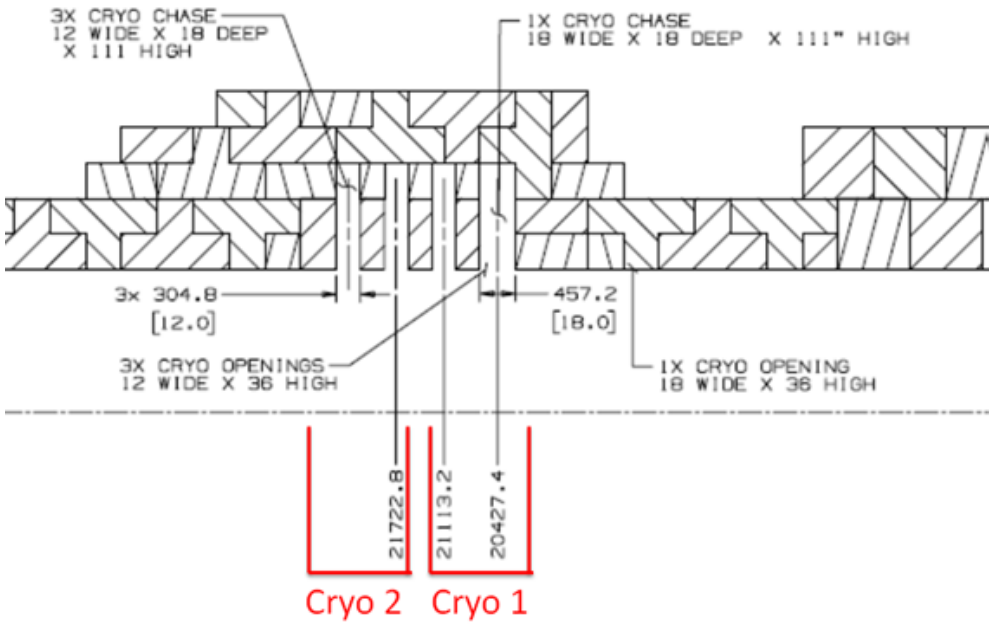

Figure 20: Drawing of the Four Cryogenic Penetrations at floor level.

than the limit reported in Table 1.

9.2 Dose rate at the exit of the Four South-East Cryo Penetrations during an accident

Figure 22 shows the dose at the exit of the Cryo-1 and Cryo-2 Penetrations as a function of the position of the beam loss along the beamline. For both Penetrations the highest dose is achieved when the beam is lost near the penetrations, at an energy of 2.1 MeV. In such cases, the dose at the exit of the penetrations is on the order of $1.4 \cdot 10^{-4}$ mrem/s which is negligible. The corresponding Sullivan Angles are reported in Figure 23.

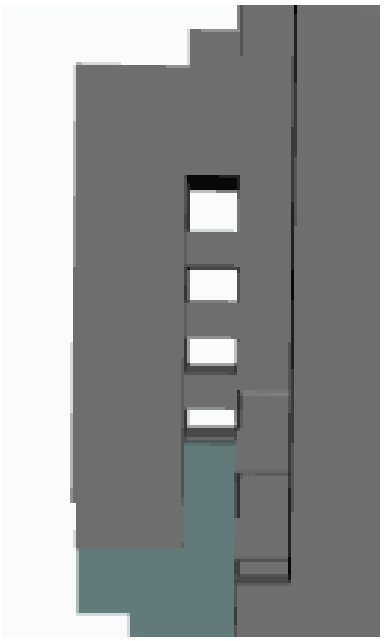

Figure 21: Exit of the Four Cryogenic Penetrations as seen from the Roof.

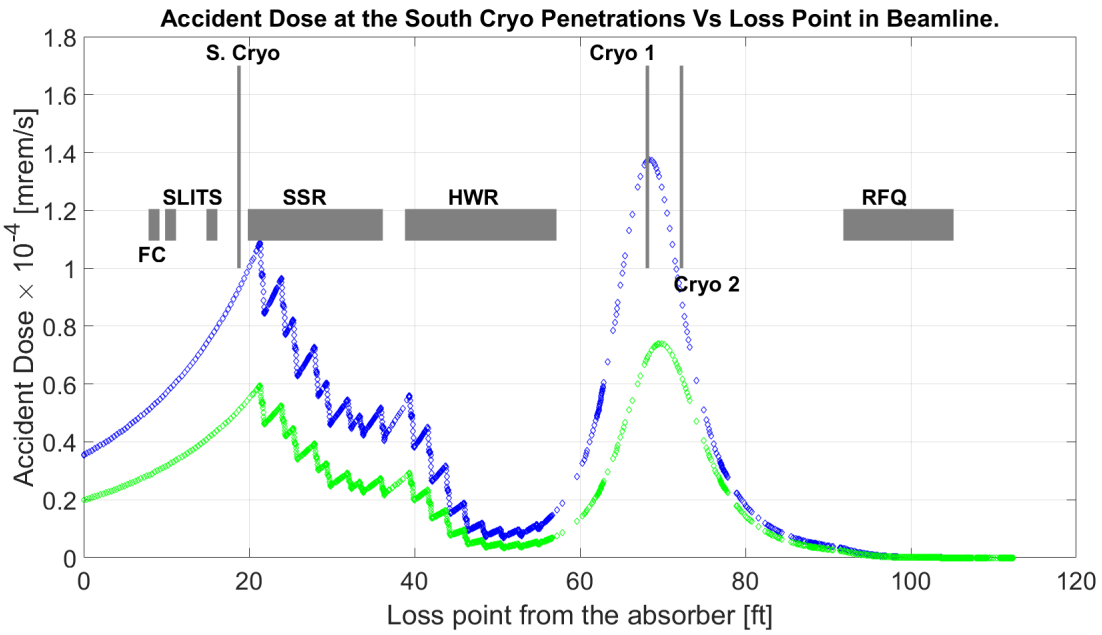

Figure 22: Accident dose at the exit of the Cryo-1 (blue) and Cryo-2 (green) Penetrations as a function of the position of the beam loss along the beamline.

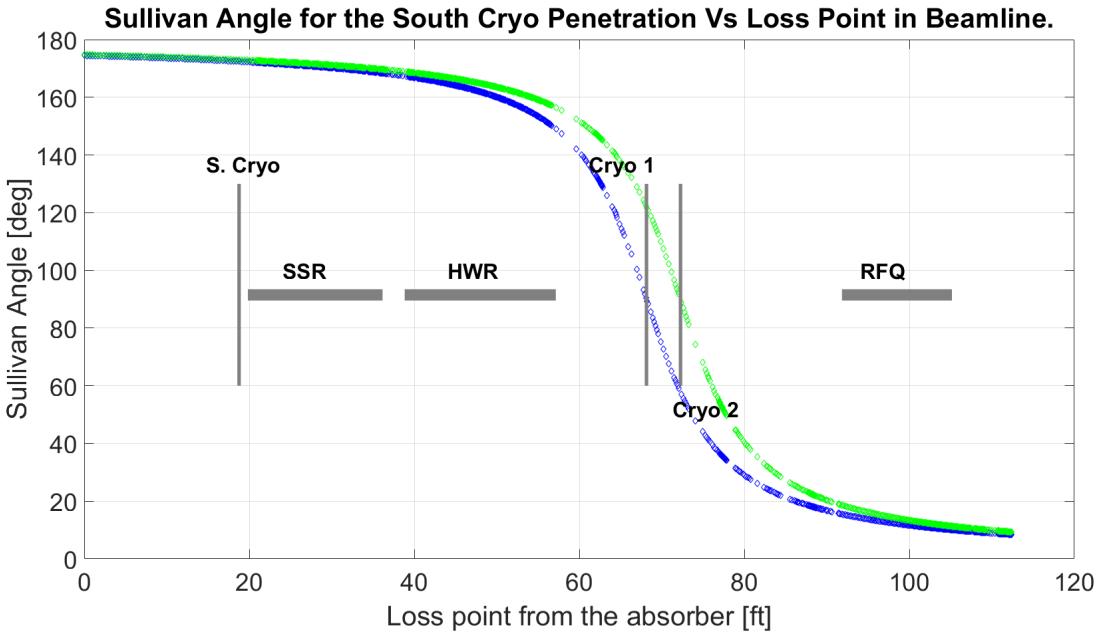

Figure 23: Sullivan Angle at the entrance of the Cryo-1 (blue) and Cryo-2 (green) Penetrations as a function of the position of the beam loss along the beamline.

10 Penetrations Block Section

Figure 24 shows the location of the 28 East Penetrations (EP01 to EP28) and the 28 West Penetrations (WP01 to WP28). The penetrations are circular cylinders of 2 ft long and start 3 ft below the roof level (7.5 ft from the floor level). As indicated in Figure 24, most of the circular apertures have a diameter of 4.5 in and 8 have a diameter of 10.8 in. The exits of the penetrations are shown in Figure 25(a) and Figure 25(b).

10.1 Dose rate at the exit of each Penetration Block Section under normal operation

Figures 26 and 27 show the estimated dose at the entrance of each East and West Penetration with radiation from the absorber under normal operation. The reported dose considers the Geometric Correction Factor of Equation 5 but does not consider shielding at the absorber.

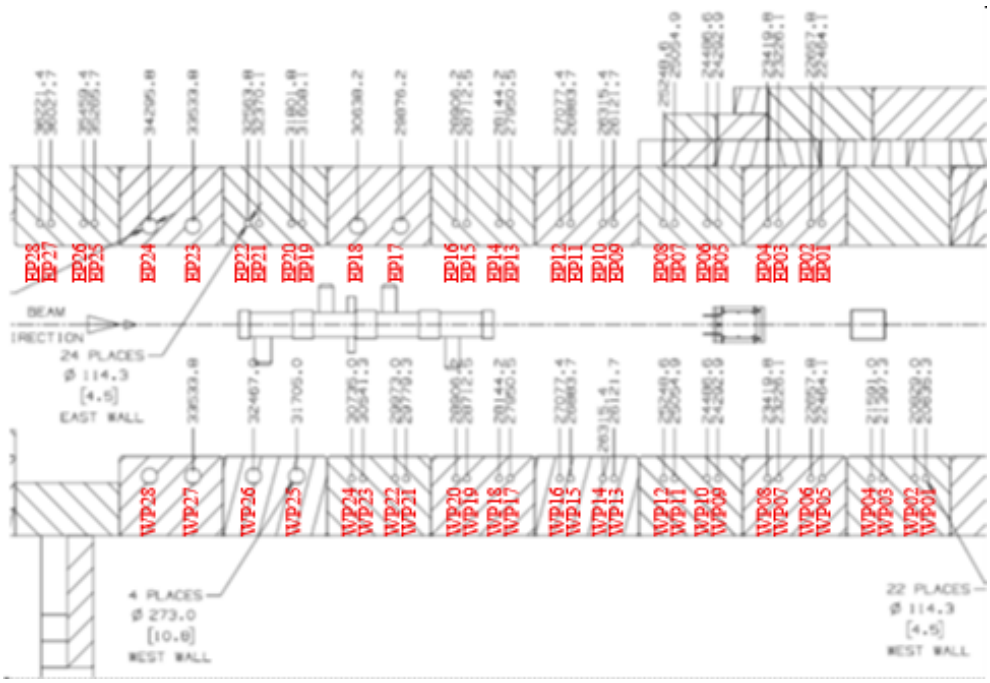

Figure 24: Penetration Block Section showing the location of the 28 East and 28 West Penetrations

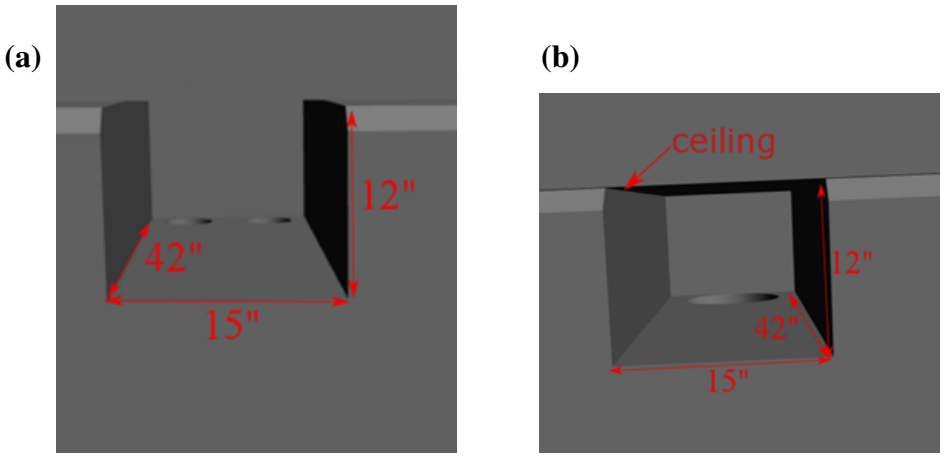

Figure 25: Exit of (a) the 4.5 in Penetrations and (b) the 10.8 in Penetrations Block Sections.

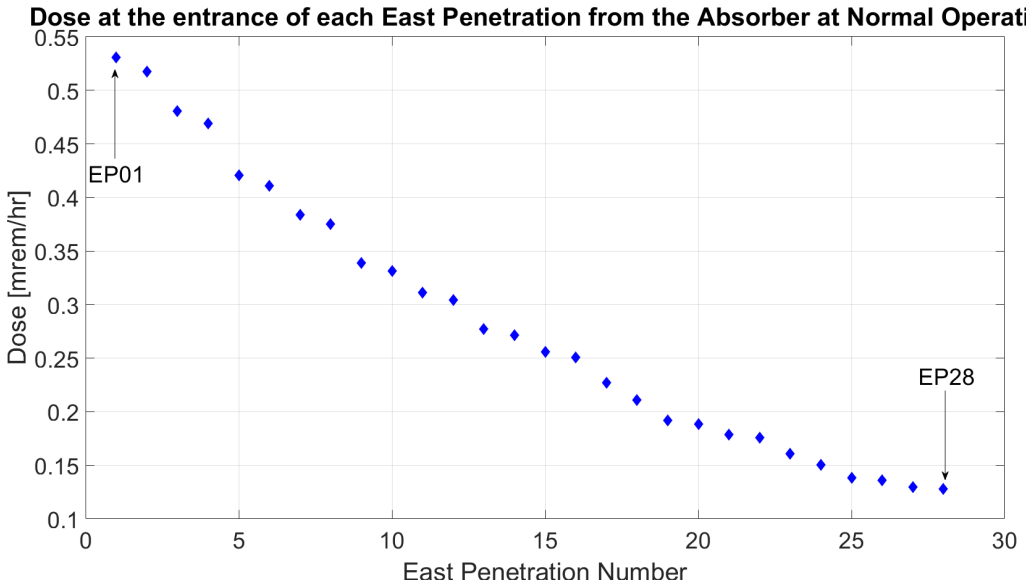

Figure 26: Radiation Dose from the absorber at the entrance of each East Penetration under normal operation. No shielding has been considered around the absorber.

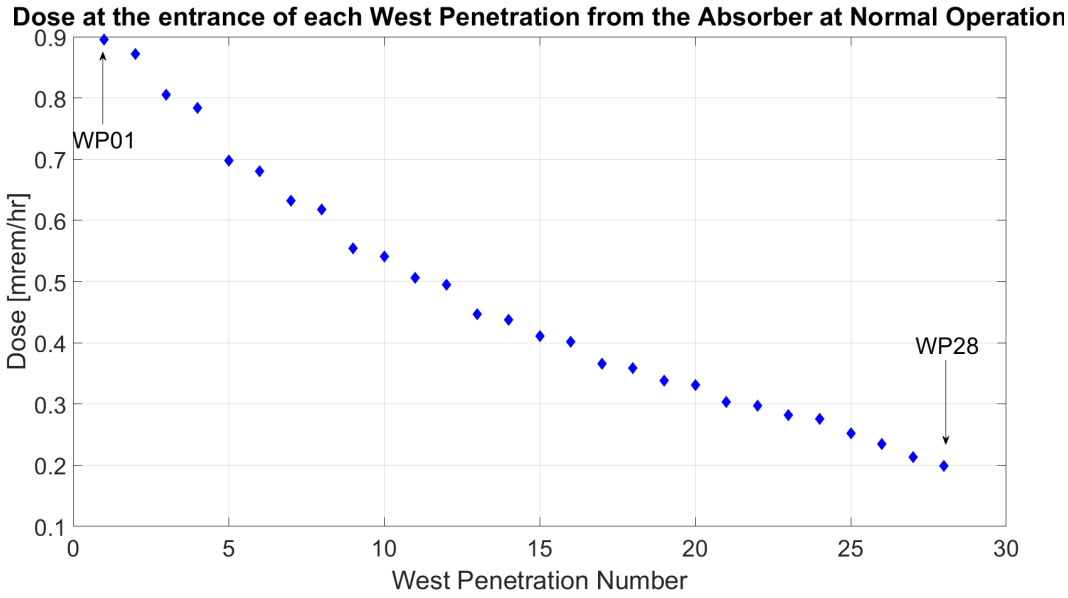

Figure 27: Radiation Dose from the absorber at the entrance of each West Penetration under normal operation. No shielding has been considered around the absorber.

Leg-1 of the 4.5 in penetrations have an attenuation factor of $3.56 \cdot 10^{-2}$. Leg-1 of the 10.8 in penetrations have an attenuation factor of $12.84 \cdot 10^{-2}$. As indicated in Figure 25(a) and Figure 25(b), each penetration exits through a Leg-2 of 1.25 ft width, 1 ft high and 3.5 ft length making an attenuation $5.9 \cdot 10^{-3}$. Tables 2 and 3 show the dose at the exit of each East and West penetration after attenuation though Legs-1 and Legs-2. Since the exit of the penetrations are near to each other, K. Vaziri suggested to add the radiation of 4 consecutive 4.5 in penetrations and 2 consecutive 10.5 in penetrations to monitor the radiation dose which is indicated in the third column of Tables 2 and 3. The radiation dose under normal operation stays below $7 \cdot 10^{-4}$ mrem/hr which is about 350 times lower than the 0.25 mrem/hr limit. Furthermore, considering the absorber shielding (with 1 in steel and 1.5 ft of concrete) will bring another $6.4 \cdot 10^{-3}$ attenuation.

10.2 Dose rate at the exit of each Penetration Block Section during an accident

Tables 4 and 5 show the maximum dose at each East and West Penetrations during an accident. The sum of 4 consecutive 4.5 in penetration and 2 consecutive 10.8 in penetration is shown on the third column of the Tables and the reported dose is negligible, at a maximum of $1.4 \cdot 10^{-4}$ mrem/s.

11 North Low Energy Labyrinth

A drawing of the North Low Energy Labyrinth is shown in Figure 28. The labyrinth is a 3-Legs labyrinth with a height of 7.5 ft throughout the labyrinth.

11.1 Dose rate at the exit of the North Low Energy Labyrinth during normal operation

Figure 28 shows that the center of Leg-1 is located at 38258.2 mm from the absorber, about 126 ft. The Sullivan Angle from the absorber to the entrance of Leg-1 is about 177° and the entrance of Leg-1 is located at $R = 6$ ft. Equation 1 predicts that the dose from the absorber at the entrance of Leg-1 is about 19 mrem/hr. This dose of 19 mrem/hr does consider the Geometric Correction Factor of Equation 5 and does not consider any

East Penetrations	Dose at penetration exits Under normal operation [mrem/hr]	Dose at successive penetrations Under normal operation [mrem/hr]
EP01	1.1E-04	
EP02	1.1E-04	
EP03	1.0E-04	
EP04	9.8E-05	4.2E-4
EP05	8.8E-05	
EP06	8.6E-05	
EP07	8.0E-05	
EP08	7.9E-05	3.3E-4
EP09	7.1E-05	
EP10	6.9E-05	
EP11	6.5E-05	
EP12	6.4E-05	3.8E-4
EP13	5.8E-05	
EP14	5.7E-05	
EP15	5.4E-05	
EP16	5.3E-05	3.7E-4
EP17	1.7E-04	
EP18	1.6E-04	3.3E-4
EP19	4.0E-05	
EP20	3.9E-05	
EP21	3.7E-05	
EP22	3.7E-05	1.5E-4
EP23	1.2E-04	
EP24	1.1E-04	2.4E-4
EP25	2.9E-05	
EP26	2.9E-05	
EP27	2.7E-05	
EP28	2.7E-05	1.1E-4

Table 2: Radiation dose from the absorber at the exit of each East Penetration Block Section under normal operation. No absorber shielding is considered. The right column shows the sum of 4 consecutive 4.5 in or 2 consecutive 10.8 in penetrations.

West Penetrations	Dose at penetration exits Under normal operation [mrem/hr]	Dose at successive penetrations Under normal operation [mrem/hr]
WP01	1.9E-04	
WP02	1.9E-04	
WP03	1.7E-04	
WP04	1.6E-04	7.0E-4
WP05	1.5E-04	
WP06	1.4E-04	
WP07	1.3E-04	
WP08	1.3E-04	5.5E-4
WP09	1.2E-04	
WP10	1.1E-04	
WP11	1.1E-04	
WP12	1.0E-04	4.4E-4
WP13	9.4E-05	
WP14	9.2E-05	
WP15	8.6E-05	
WP16	8.4E-05	3.6E-4
WP17	7.7E-05	
WP18	7.5E-05	
WP19	7.1E-05	
WP20	6.9E-05	2.9E-4
WP21	6.4E-05	
WP22	6.3E-05	
WP23	5.9E-05	
WP24	5.8E-05	2.4E-4
WP25	1.9E-04	
WP26	1.7E-04	3.7E-4
WP27	1.6E-04	
WP28	1.5E-04	3.1E-4

Table 3: Radiation dose from the absorber at the exit of each West Penetration Block Section under normal operation. No absorber shielding is considered. The right column shows the sum of 4 consecutive 4.5 in or 2 consecutive 10.8 in penetrations.

East Penetrations	Dose at penetration exits Under accident conditions [mrem/s]	Dose at successive penetrations Under accident conditions [mrem/s]
EP01	2.2E-05	
EP02	2.2E-05	
EP03	2.1E-05	
EP04	2.1E-05	8.6E-5
EP05	1.9E-05	
EP06	1.8E-05	
EP07	1.7E-05	
EP08	1.6E-05	6.7E-5
EP09	1.6E-05	
EP10	1.6E-05	
EP11	2.3E-05	
EP12	2.3E-05	8.0E-5
EP13	2.2E-05	
EP14	2.1E-05	
EP15	1.9E-05	
EP16	1.9E-05	8.6E-5
EP17	5.5E-05	
EP18	4.7E-05	1.0E-4
EP19	1.1E-05	
EP20	1.0E-05	
EP21	4.6E-06	
EP22	4.5E-06	3.0E-4
EP23	1.6E-05	
EP24	1.5E-05	3.1E-5
EP25	4.1E-06	
EP26	4.1E-06	
EP27	4.0E-06	
EP28	4.0E-06	1.6E-5

Table 4: Radiation at the exit of each East Penetration Block Section after an accident. The right column shows the sum of 4 consecutive 4.5 in or 2 consecutive 10.8 in penetrations.

West Penetrations	Dose at penetration exits Under accident conditions [mrem/s]	Dose at successive penetrations Under accident conditions [mrem/s]
WP01	3.7E-05	
WP02	3.6E-05	
WP03	3.4E-05	
WP04	3.4E-05	1.4E-4
WP05	3.2E-05	
WP06	3.2E-05	
WP07	3.1E-05	
WP08	3.1E-05	1.3E-4
WP09	2.9E-05	
WP10	2.9E-05	
WP11	1.6E-05	
WP12	1.6E-05	9.1E-5
WP13	1.5E-05	
WP14	1.5E-05	
WP15	1.5E-05	
WP16	1.5E-05	6.0E-5
WP17	1.4E-05	
WP18	1.4E-05	
WP19	1.4E-05	
WP20	1.4E-05	5.5E-5
WP21	8.3E-06	
WP22	8.3E-06	
WP23	8.0E-06	
WP24	8.0E-06	3.3E-5
WP25	2.8E-05	
WP26	2.7E-05	5.5E-5
WP27	2.6E-05	
WP28	2.5E-05	5.0E-5

Table 5: Radiation at the exit of each West Penetration Block Section after an accident. The right column shows the sum of 4 consecutive 4.5 in or 2 consecutive 10.8 in penetrations.

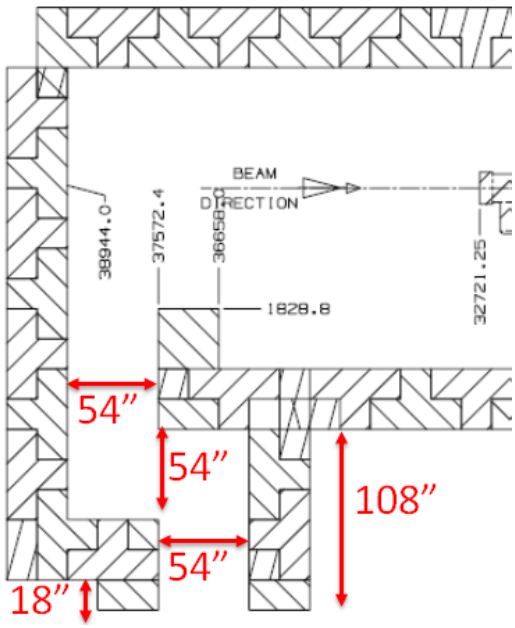

Figure 28: Layout of the North Low Energy Labyrinth.

shielding around the absorber. Leg-1 of the labyrinth has a width of 4.5 ft, a height of 7.5 ft and a length of 8.25 ft. The cross-sectional area of the first leg is $A_1 = 33.75$ ft^2. According to Equation 7, $\delta_1 = 8.25/(\sqrt{33.75}) = 1.4$ and the attenuation factor through Leg-1 of the south labyrinth is $[1.4/(1.4+1.4)]^2 = 0.25$. The width of Leg-2 is 4.5 ft, the height 7.5 ft and the length 4.5 ft. The cross-sectional area of the second leg is $A_2 = 33.75$ ft^2. According to Equation 8, $\delta_2 = 4.5/(\sqrt{33.75}) = 0.77$ and the attenuation factor through Leg-2 of the south labyrinth is 0.1.

Leg-3 of the labyrinth has a width of 4.5 ft, a height of 7.5 ft and a length of 6.75 ft. The cross-sectional area of the first leg is $A_3 = 33.75$ ft^2. According to Equation 8 $\delta_3 = 6.75/(\sqrt{33.75}) = 1.17$ and the attenuation factor through Leg-3 is 0.06. The dose at the exit of North Low Energy Labyrinth from absorber radiation is estimated at 19 mrem/hr$\times 0.25 \times 0.1 \times 0.06 = 0.03$ mrem/hr without consideration of shielding at the absorber, which is about 8 times lower than the limit reported in Table 1.

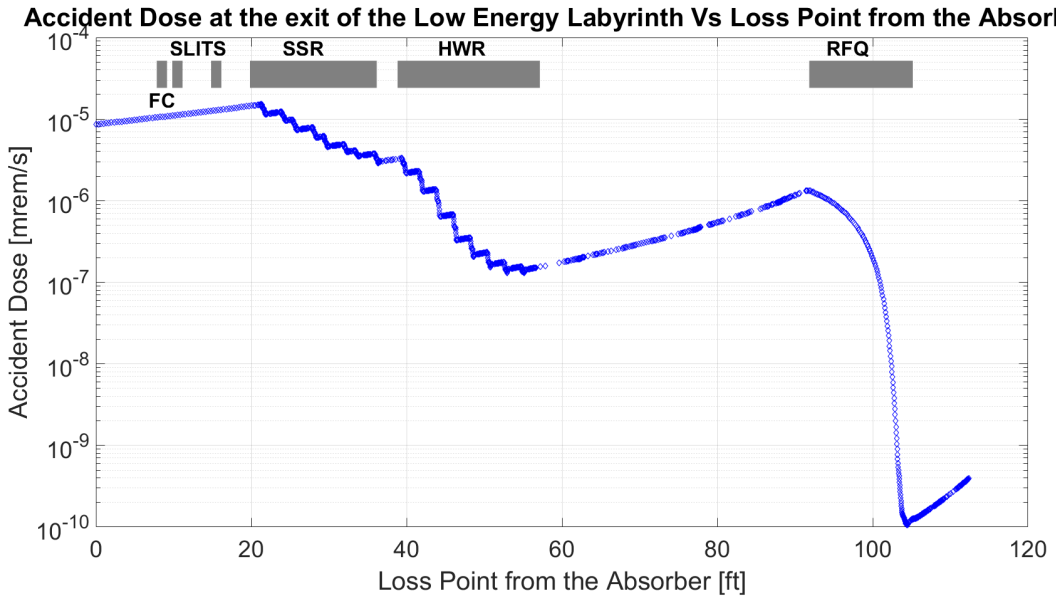

Figure 29: Accident dose at the exit of the North Low Energy Labyrinth as a function of the beam loss along the beamline.

11.2 Dose rate at the exit of the North Low Energy Labyrinth after an accident

Figure 29 shows that in the event of an accident the dose rate at the exit of the North Low Energy Labyrinth is negligible, in the order of 10^{-5} mrem/s for a beam lost at 25 MeV at the exit of the SSR cryomodule. The corresponding Sullivan Angle is reported in Figure 30.

12 Roof

The roof is 3 ft thick throughout the entire enclosure except for the interruptions due to penetrations. Note that in the previous shielding assessment study documented in Ref. [8] the roof thickness was 3 ft upstream of the enclosure up to the HWR and 4.5 ft downstream up to the high energy end.

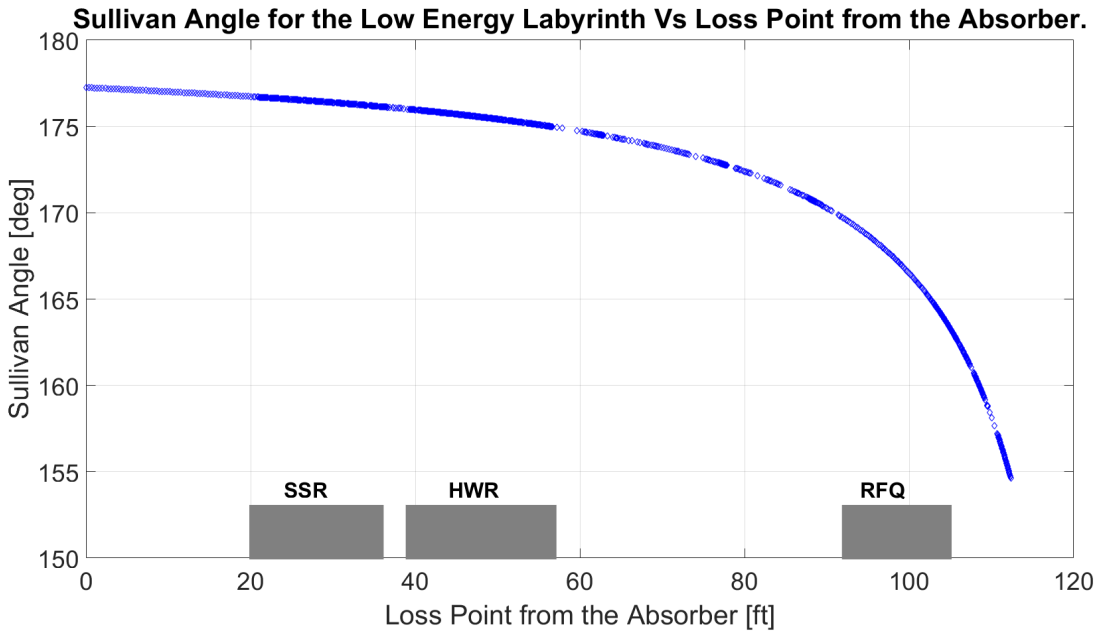

Figure 30: Sullivan Angle for the North Low Energy Labyrinth as a function of the position of the beam loss along the beamline.

12.1 Dose rate at the top of the roof during normal operation

The dose rate on the enclosure ceiling directly above the beam absorber ($\theta_s = 90°$) is about $2.5 \cdot 10^5$ mrem/hr according to Equation 1. As previously mentioned, the 1 in steel shielding at the absorber is attenuating the dose by a factor of about 0.4. The top of the absorber is shielded by 3 ft of concrete making an attenuation of about $2.7 \cdot 10^{-4}$ and the 3 ft roof shielding provides the same attenuation. Therefore, the dose rate at the top of the roof is estimated to be: $2.5{\cdot}10^5 \times 0.4 \times 2.7{\cdot}10^{-4} \times 2.7{\cdot}10^{-4} = 7{\cdot}10^{-3}$ mrem/hr. In the case we consider a conservative 1.5 ft of concrete shielding at the absorber, the dose rate at the top of the cave roof becomes $2.5 \cdot 10^5 \times 0.4 \times 1.6 \cdot 10^{-2} \times 2.7 \cdot 10^{-4} = 0.4$ mrem/hr which is still within the limit allowed for a roof of enclosure (between 0.25 and 5 mrem/hr) as mentioned in Table 1. Figure 31 shows the dose on the top of the roof along the beamline from the absorber.

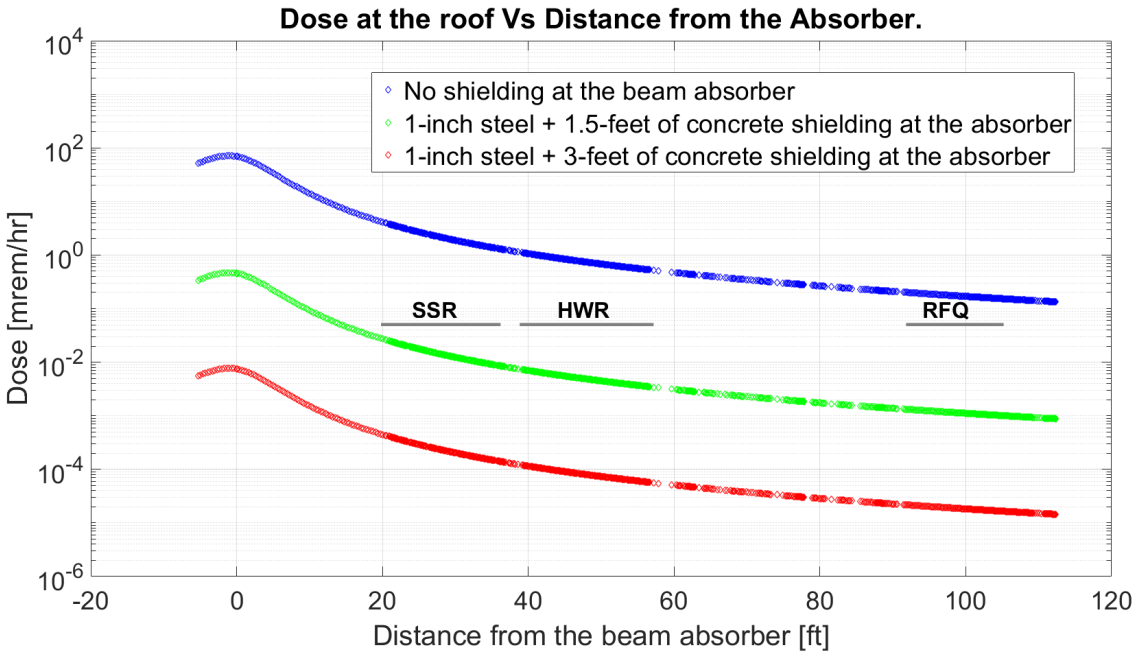

Figure 31: Dose from the absorber at the top of the roof under normal beam operation.

12.2 Dose rate at the top of the roof after an Accident

Figure 32 shows the expected accident dose at the top of the roof for a beam loss anywhere along the beamline. The dose reported in Figure 32 is calculated using Equations 1 to 9 at the vertical of the loss point on the top of the roof. A beam loss at 25 MeV (exit of the SSR cryomodule up to the absorber entrance) is expected to generate an accident dose at the roof of about 19×10^{-3} mrem/s. A beam loss occuring about 28 ft upstream the absorber (about half-way inside the SSR cryomodule) is expected to generate a dose at the roof of about 2.8×10^{-3} mrem/s (corresponding to about 10 mrem in 1 hour) and a beam loss occuring at about 29.5 ft upstream the absorber is expected to generate a dose at the roof of about 1.4×10^{-3} mrem/s (corresponding to about 5 mrem in 1 hour). A beam loss at the start of the SSR cryomodule located about 36 ft from the absorber and where the beam energy is 10 MeV will generate a dose at the roof of about 4.6×10^{-4} mrem/s.

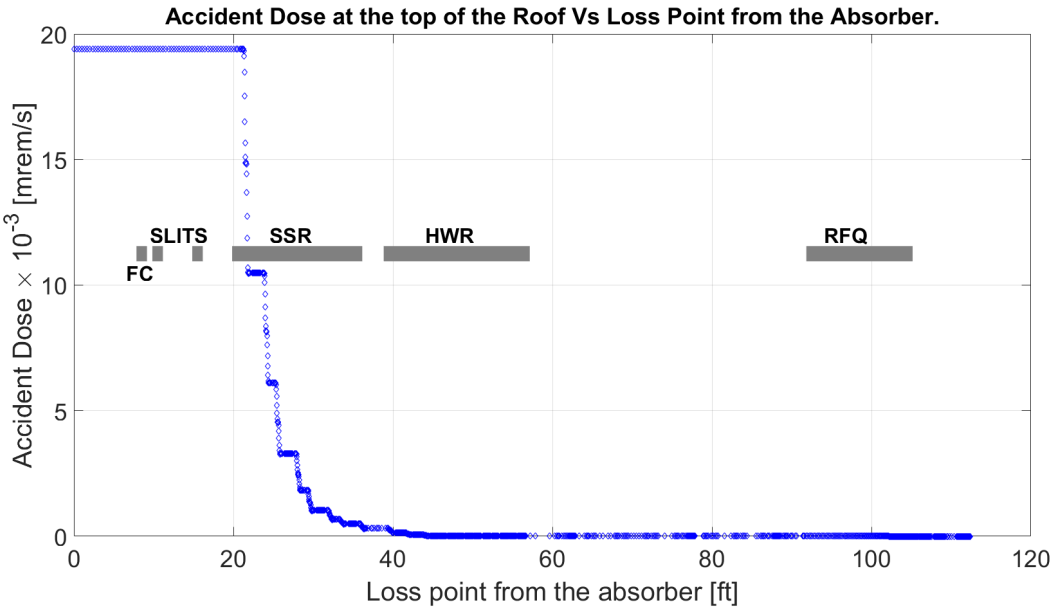

Figure 32: Accident dose at the top of the roof as a function of the beam loss afrom the absorber.

12.3 MARS dose rate at the top of the roof

Figure 33 shows the estimated MARS total effective dose rate at the roof for a beam power of 550 W at the absorber. MARS predicts a maximum effective does rate of 1.3 mrem/hr of the same order of magnitude than the 0.6 mrem/hr calculated analytically and reported in Section 12.1.

13 Walls

The walls of the enclosure are 3 ft thick from the low energy section up the middle of the HWR cryomodule and 6 ft thick downstream. As a conservative approach, we consider the radiation at the outside of the East Walls which are closer to the beamline (6 ft) than the West Walls (9 ft).

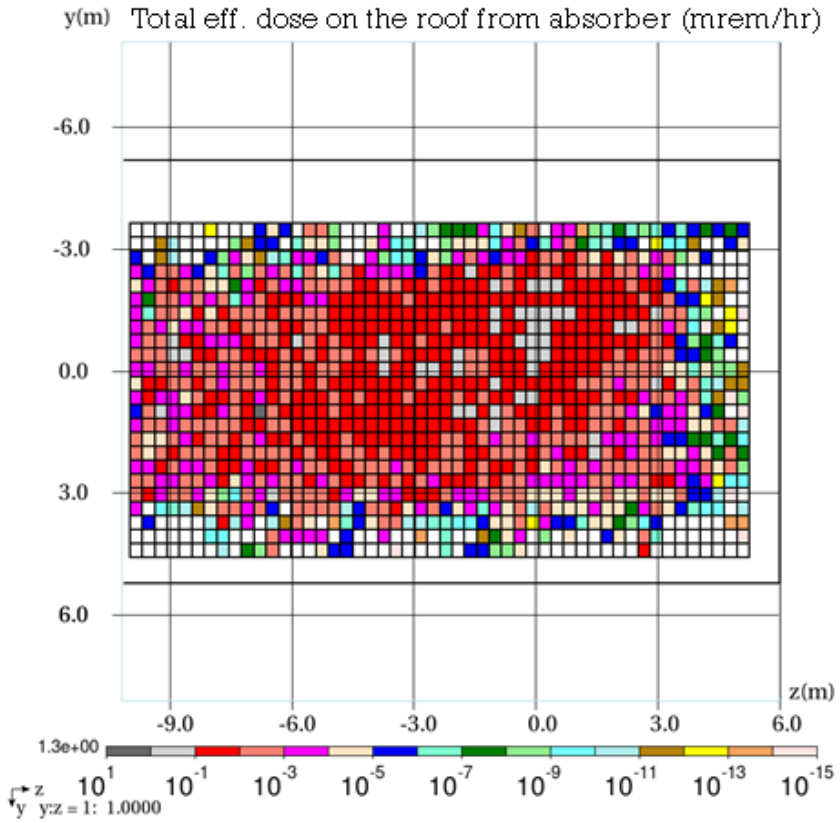

Figure 33: MARS Total Effective Dose from the absorber at the top of the roof under normal beam operation.

13.1 Dose rate at 6 ft and 3 ft East-Walls under normal operation

The East Walls are located at $R = 6$ ft from the absorber. Considering $D = 0$, $r = 6$ ft, $\theta_s = 90$ deg, E=0.025 GeV, the dose rate in the inside part of the East Wall is $2.5 \cdot 10^5$ mrem/hr. The East side of the absorber is shielded by 1.5 ft of concrete and 1 in of steel. The East Walls in the high energy part of the enclosure provide an additional 6 ft of shielding or an attenuation of $7.3 \cdot 10^{-8}$. The dose rate at the outside East Wall is expected to be: $2.5 \cdot 10^5 \times 0.4 \times 0.016 \times 7.3 \cdot 10^{-8} = 1.2 \cdot 10^{-4}$ mrem/hr which is about 3 orders of magnitude lower than the limit reported in Table 1. Figures 34 and 35 show the radiation from the absorber outside the 6 ft and 3 ft walls for three different scenarios of shielding around the absorber. Even without any shielding around the absorber, the 6 ft thick East Walls provide an attenuation enough ($7.3 \cdot 10^{-8}$) to stay below the 0.25 mrem/hr limit.

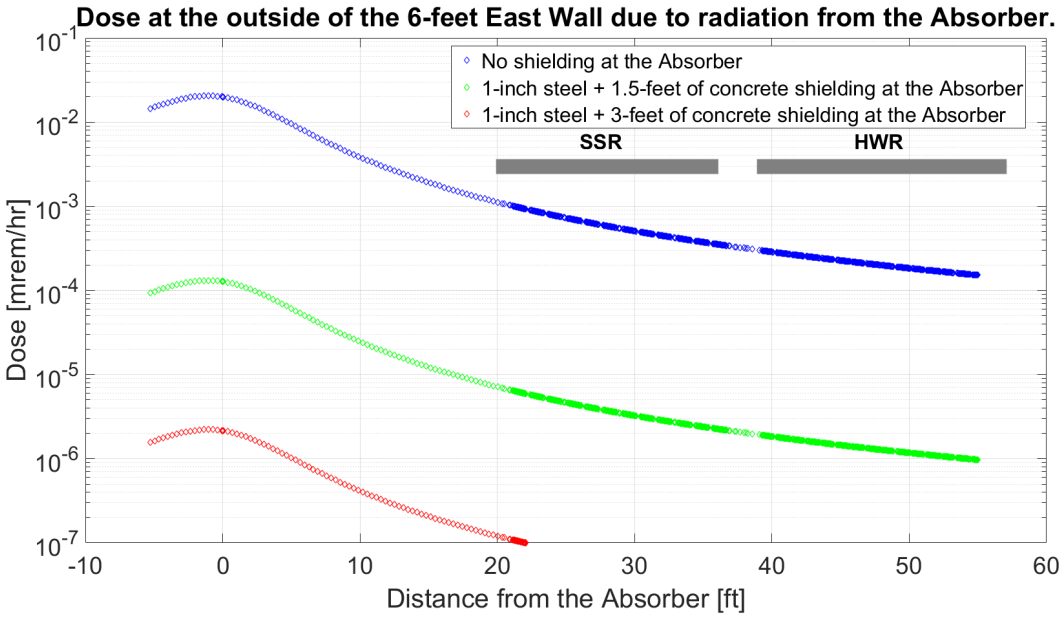

Figure 34: Dose outside the 6 ft East Wall due to radiation from the absorber under normal operation.

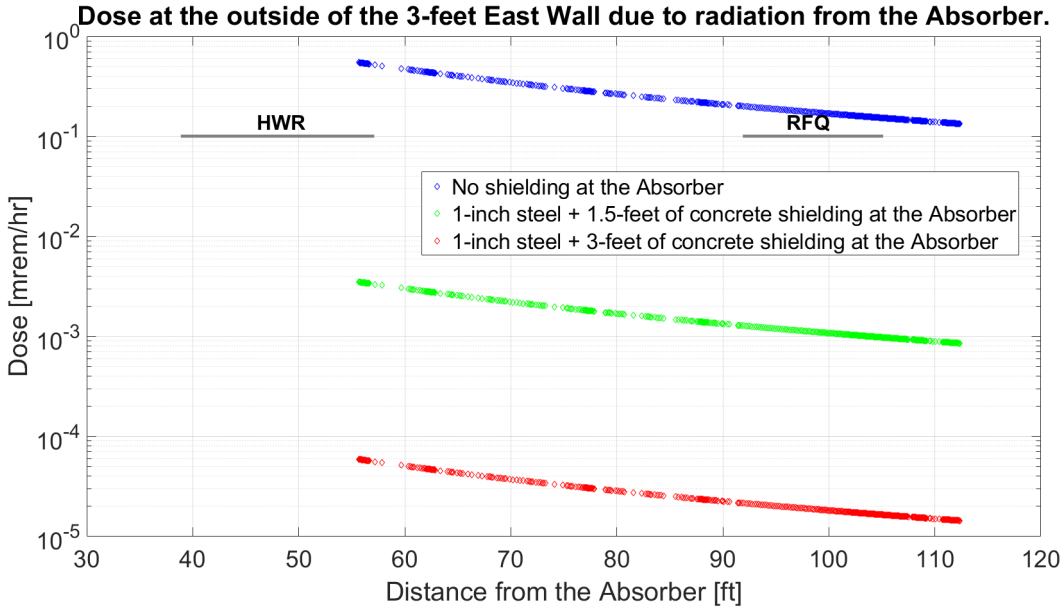

Figure 35: Dose outside the 3 ft East Wall due to radiation from the absorber under normal operation.

For the 3 ft thick walls, Figure 35 shows that a conservative 1 in steel and 1.5 ft concrete shielding around the absorber keeps the radiation dose below $3.5 \cdot 10^{-3}$ mrem/hr outside the 3 ft walls, which about 80 times lower than the limit.

13.2 Dose rate at 6 ft and 3 ft East-Walls after an accident

If a 25 MeV beam is lost before reaching the absorber, the maximum accident dose in the inside of the 6 ft walls will be about 70 mrem/s. Outside the 6 ft wall this dose will reduce to $70 \times 7.3 \cdot 10^{-8} = 5 \cdot 10^{-6}$ mrem/s. In the case the beam is lost in the region of the 3 ft walls, the accident dose rate is expected to not exceed $2.0 \cdot 10^{-6}$ mrem/s. These dose are significantly lower than the accident dose limit presented in Table 1.

14 Residual Dose Rate Analysis from MARS

Figure 36 shows the estimated residual dose rates in mrem/hr around the absorber after 30 days of irradiation and 1 day of cooling. This Figure shows that the highest residual dose rate at the outer surface of the concrete shielding blocks surrounding the absorber is around 10 mrem/hr. The corresponding error on this residual dose rate reported by MARS is on the order of $3.9 \cdot 10^{-3}$ mrem/hr.

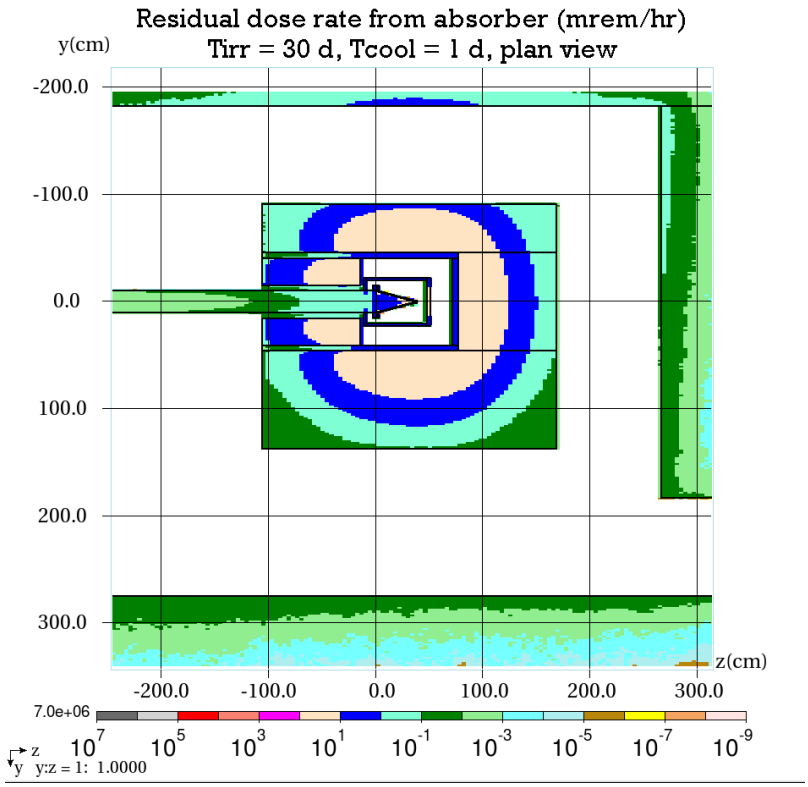

Figure 36: Residual dose rates in mrem/hr at the absorber and surrounding concrete shielding after 30 days of irradiation and 1 day of cool down under normal operation.

15 HEBT Slit

Two pairs of slits are expected to be installed in the High Energy Beam Transport (HEBT) line. The purpose of these slits is horizontal and vertical phase space reconstruction. At the writing time of this document, the slits have not been designed. Nevertheless, each pair of slits is expected to comprise a horizontal and vertical slit made of TMZ plates of 20 mm high, 20 mm wide and 2 mm thick in the beam direction. The slit aperture is expected to be in the order of 200 μm. As indicated in Figure 37, the first pair of slits is expected to be located 4337.6 mm from the absorber cone entrance and is expected to intercept most of the beam. The second pair of slits is expected to be located 1394.2 mm downstream of the first pair of slits (2943.4 mm from the entrance of the absorber cone). To perform a phase space reconstruction, the beam will be sampled by Slit1 (horizontal or vertical)

and each beamlet sampled by Slit 2 (horizontal or vertical). An insertable Faraday Cup located 320.7 mm downstream of Slit 2 will collect the remaining beam leaving Slit 2. The preferable mode of operation during a phase space reconstruction is 2 mA, 10 μs, 20 Hz at 25 MeV corresponding to $2.5 \cdot 10^{12}$ H^- per second. The heat load on Slit1 is about 10 W and each scan is excepted to take about 20 minutes to complete. Estimates have shown that a maximum of 10% of the initial beam is expected to go through Slit1 and reach Slit2 and another 10% is expected to go through Slit2 and reach the Faraday Cup. Therefore a maximum of 1% of the initial beam is expected to be intercepted by the Faraday Cup during a scan.

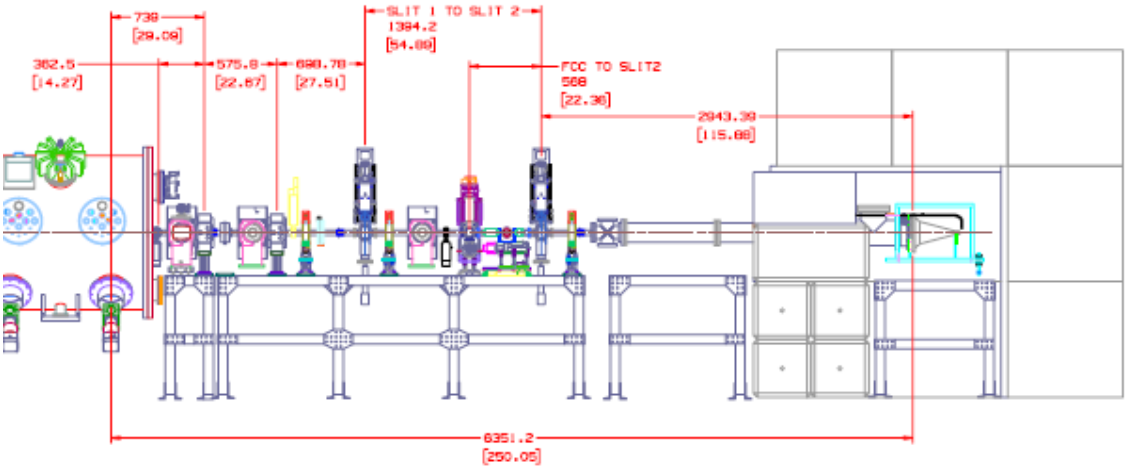

Figure 37: Layout of the HEBT Beamline.

15.1 MARS radiation calculation for Slit1

Figure 38 shows a plan view and Figure 39 shows an elevation view of the MARS total effective dose from Slit1 for $1.375 \cdot 10^{14}$ H^- at 25 MeV corresponding to a beam power of 550 W. As reported in Section 15, the HEBT slits are expected to operate at a power 55 times lower than reported in Figure 38 and Figure 39.

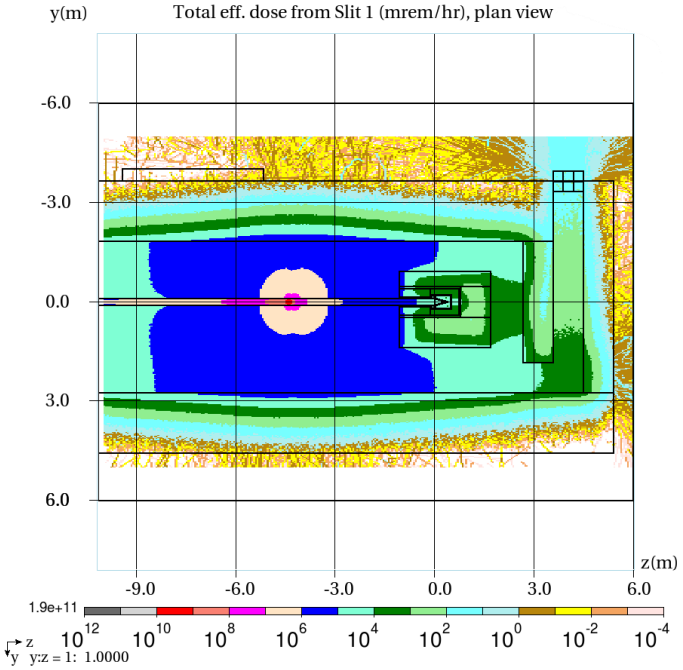

Figure 38: MARS Total Effective Dose from Slit1, Plan View.

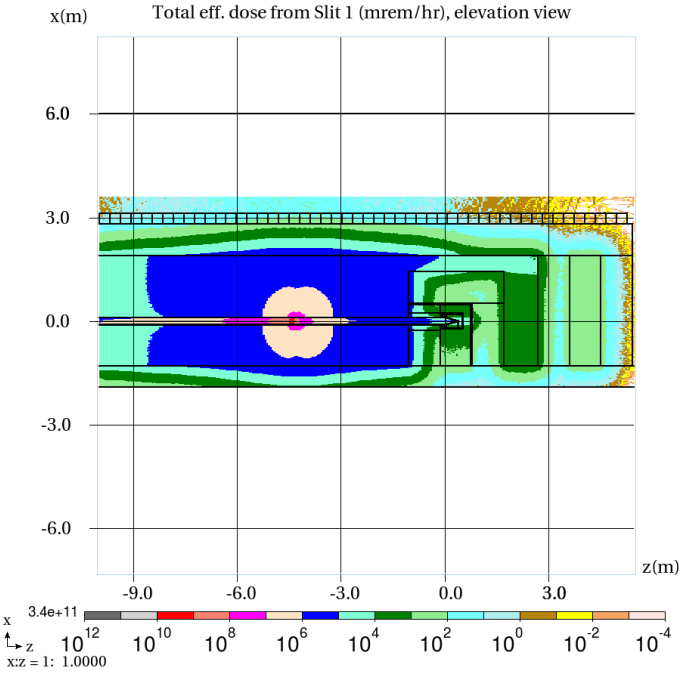

Figure 39: MARS Total Effective Dose from Slit1, Elevation View.

15.2 Dose rate at the exit of the South Emergency Exit Labyrinth for the beam intercepted by Slits1

The following parameters can be deduced from Figure 37 concerning the location of Slit1 and South Emergency Exit Labyrinth: $R = 23$ ft, $D = 7.5$ ft, $r = 24.4$ ft, $\theta_s = 18.06°$ and E=0.025 GeV.

Taking the above parameters and $1.375 \cdot 10^{14}$ H^- at 25 MeV, Equation 1 reports that the dose at the entrance of Leg-1 is $2.6 \cdot 10^4$ mrem/hr considering the Geometric Correction Factor correction given in Equation 6. As indicated in Section 7.1, the attenuation factor is 0.38 for Leg-1 of the South Emergency Exit Labyrinth and $7.6 \cdot 10^{-3}$ for Leg-2. Therefore, the dose at the exit of the South Emergency Exit labyrinth without any attenuation around Slit1 is given by the dose at the labyrinth entrance times the attenuation of Leg-1 and Leg-2 which equals: $2.6 \cdot 10^4 \times 0.38 \times 7.6 \cdot 10^{-3} = 75$ mrem/hr. Figure 40 shows the MARS Total Effective Dose from Slit1 at the South Emergency Exit Labyrinth for $1.375 \cdot 10^{14}$ H^- at 25 MeV on Slit1. MARS reports a maximum dose of 70 mrem/hr, similar to the dose rate of 75 mrem/hr predicted analytically.

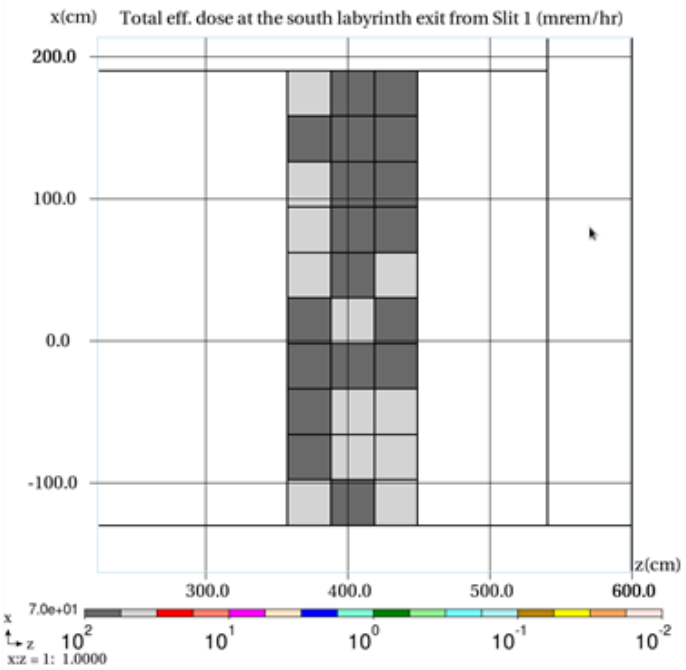

Figure 40: MARS Total Effective Dose from Slit1 at the South Emergency Exit Labyrinth.

15.3 Dose rate at the exit of the South Emergency Exit Labyrinth Short-Circuits for the beam intercepted by Slit1

As indicated in Figure 11, two short-circuits should be considered for the South Emergency Exit Labyrinth. The first one (noted short-Circuit-1 in Figure 11) allows the radiation from Leg-1 to reach the outside of the enclosure through the 3 ft South Wall. As discussed in Section 15.2 the dose at the entrance of Leg-1 of the labyrinth is $2.6 \cdot 10^4$ mrem/hr considering the Geometric Correction Factor correction factor given in Equation 6. Attenuation through Leg-1 is estimated at 0.38. The 3 ft South Wall brings another $2.7 \cdot 10^{-4}$ attenuation. Therefore, the dose at the exit of the 3 ft wall can be estimated at $2.6 \cdot 10^4 \times 0.38 \times 2.7 \cdot 10^{-4} = 2.7$ mrem/hr (Short-Circuit1).

The second short-circuit (noted Short-Circuit-2 in Figure 11) allows radiation to reach the outside gate of the South Emergency Exit Labyrinth through the 3 ft wall located just behind the absorber and through 12 ft of the Labyrinth leg. Equation 1 estimates the radiation from the absorber on the inside part of the 3 ft wall to be about $3.4 \cdot 10^4$ mrem/hr. Considering the 3 ft wall brings $2.7 \cdot 10^{-4}$ attenuation factor and the 12 ft Leg give another 0.1 attenuation factor, the estimated dose rate at the South Emergency Exit Labyrinth gate through the Short-Circuit-2 is estimated to be $3.4 \times 10^4 \times 2.7 \cdot 10^{-4} \times 0.1 = 0.9$ mrem/hr.

15.4 Dose rate at the top of the cave enclosure 3 ft roof for the beam intercepted by Slits1

The cave ceiling is located 6.2 ft from the beamline and the roof is made of 3 ft of concrete. Equation 1 reports that the dose at the cave roof is expected to be $2.5 \cdot 10^5$ mrem/hr for $1.375 \cdot 10^{14}$ H^- at 25 MeV intercepted by Slit1. Equation 9 reports that 3 ft of concrete provides an attenuation of $2.7 \cdot 10^{-4}$. Therefore, the dose at the top of the 3 ft roof is expected to be $2.5 \cdot 10^5 \times 2.7 \cdot 10^{-4} = 67$ mrem/hr. Figure 41 reports MARS total effective dose at the roof of 88 mrem/hr for $1.375 \cdot 10^{14}$ H^- at 25 MeV, of the same order as the value obtained analytically.

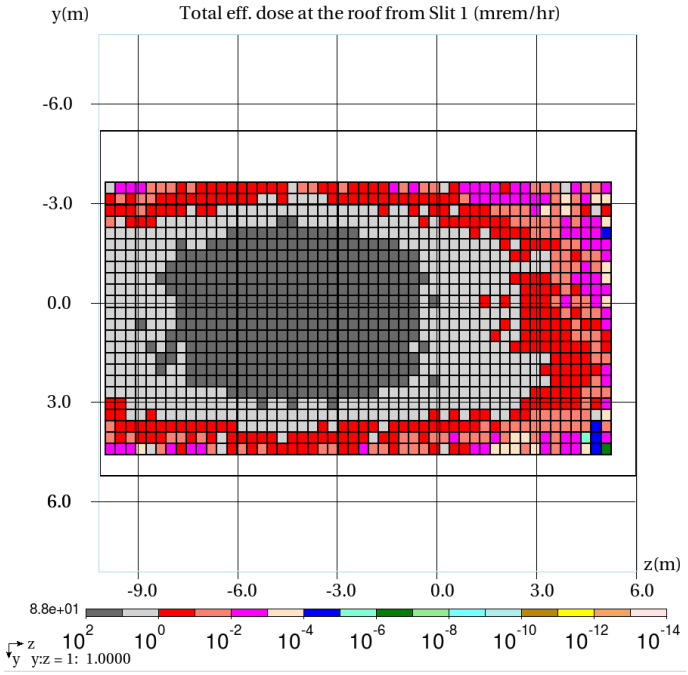

Figure 41: MARS total effective dose from Slit1 at the Top of the Roof.

15.5 Dose rate at the South-East Cryo Penetration exit for the beam intercepted by Slits1

The following parameters can be deduced from Figure 16 and Figure 37 concerning the South-East Cryo Penetration with radiation from Slit1: $R = 8.13$ ft, $D = 4.54$ ft, $r = 9.31$ ft, $\theta_s = 119°$ and E=0.025 GeV. Taking the above parameters and $1.375 \cdot 10^{14}$ H^- at 25 MeV, Equation 1 reports that the dose at the entrance of Leg-1 of the South-East Cryo Penetration is about $8.4 \cdot 10^4$ mrem/hr taking into account the Geometric Correction Factor correction given in Equation 5.

Considering attenuation factors for the South-East Cryo Penetration legs reported in Section 7.1 of 0.13 for Leg-1, $1.7 \cdot 10^{-3}$ for Leg-2 and $23.3 \cdot 10^{-3}$ for Leg-3 the expected dose rate at the exit of the South-East Cryo Penetration coming from Slit1 is expected to be: $8.4 \cdot 10^4 \times 0.13 \times 1.7 \cdot 10^{-3} \times 23.3 \cdot 10^{-3} = 4.3 \cdot 10^{-1}$ mrem/hr. Figure 42 reports a MARS total effective dose at the exit of the South-East Cryo Penetration from Slit1 operating at $1.375 \cdot 10^{14}$ H^- and 25 MeV of 5.4 mrem/hr, about one order of magnitude larger than predicted analytically.

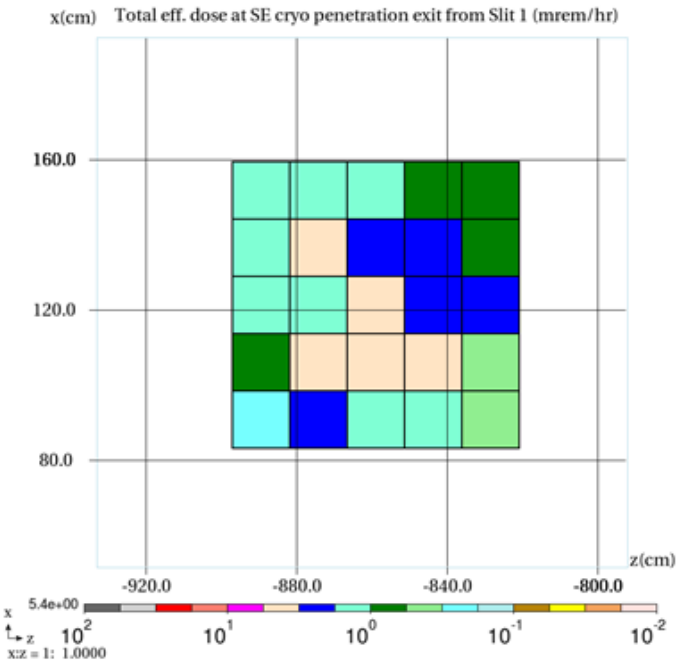

Figure 42: MARS Total Effective Dose from Slit1 at the South-East Cryo Penetration.

The Short-Circuit of the South-East Cryo Penetration is shown in Figure 16. At the exit of Leg-1, radiation can reach the outside of the enclosure through a 3 ft concrete shielding. The dose at the exit of the South-East Cryo Penetration Short-Circuit shown in Figure 16 is estimated for $1.375 \cdot 10^{14}$ H^- at 25 MeV at: $8.4 \cdot 10^4 \times 0.13 \times 2.7 \cdot 10^{-4} = 3$ mrem/hr considering an attenuation factor of $2.7 \cdot 10^{-4}$ for 3 ft concrete shielding for the Leg-1 exit.

15.6 Dose rate at the exit of the Walls for the beam intercepted by Slits1

The East 6 ft Wall is located at $R = 6$ ft from Slit1 and provides an attenuation of $7.3 \cdot 10^{-8}$. Considering, $D = 0$, $r = 6$ ft, $\theta_s = 90$ deg, E=0.025 GeV the dose rate in the inside part of the East Wall is $2.7 \cdot 10^5$ mrem/hr. The dose rate at the outside East 6 ft Wall is expected to be: $2.7 \cdot 10^5 \times 7.3 \cdot 10^{-8} = 2 \cdot 10^{-2}$ mrem/hr. The following parameters can be deduced from Figure 37 and Figure 11 concerning the East 3 ft Walls with radiation from Slit1: $R = 6$ ft, $D = 43$ ft, $r = 43.4$ ft, $\theta_s = 172°$ and E=0.025 GeV. We are considering the part of the East 3 ft Wall closer to Slit1, which is approximately at the

start of the HWR cryomodule as indicated in Figure 3. Taking the above parameters and $1.375 \cdot 10^{14}$ H^- at 25 MeV, Equation 1 reports that the dose in the inside part of the East 3 ft Wall is $3.4 \cdot 10^3$ mrem/hr. The dose rate at the outside East 3 ft Wall is expected to be: $3.4 \cdot 10^3 \times 2.7 \cdot 10^{-4} = 0.9$ mrem/hr.

16 Dose Outside of the CMTF Building from the South Emergency-Exit Labyrinth gate

As indicated in Section 7, the South Emergency-Exit Labyrinth gate is a rectangle of 3 ft width and 9 ft high. The gate is located about 80 in from the CMTF building inside East wall. We consider the wall to be about 6 in thick. Therefore a point located 8 ft away on the axis of symmetry perpendicular to the gate rectangle can be considered to be located just outside of the CMTF building East wall. According to Ref. [11], the attenuation factor 8 ft away on the axis of symmetry perpendicular to the gate rectangle is about $3.5 \cdot 10^{-2}$. Under normal operation with 550 W of power at the absorber, Section 7 reports a maximum dose at the labyrinth gate of 1.4 mrem/hr corresponding to a maximum dose of $4.9 \cdot 10^{-2}$ mrem/hr just outside of the CMTF building East wall. During normal slit operation at 10 W, Section 15 reports a maximum dose at the labyrinth gate of 1.4 mrem/hr corresponding to a maximum dose of $4.9 \cdot 10^{-2}$ mrem/hr just outside of the CMTF building East wall. In both normal operation cases, the dose just outside of the CMTF building East wall stays below the $5 \cdot 10^{-2}$ mrem/hr limit listed in Table 1 during normal operation of the injector with beam at the absorder and at the slit.

17 Muon Production

Since the mass of a muon is 105.7 MeV/c^2, it is not possible to produce them with a 25 MeV beam. No further consideration of muon production or shielding for muons is required for this PIP2IT shielding assessment .

18 Ground Water

The 25 MeV beam is below the threshold for producing H-3 and Na-22 in the soil. The cross-section reaction channels, such as neutron or barrier tunneling, are too small to amount to any significant production in the soil. Therefore, there can be no contamination of the ground waters due to PIP2IT operations. The Environmental Protection Agency defines surface water for Fermilab as waters that enter and leave the Laboratory site. Concentration limits for the surface water are 1900 pCi/ml for tritium and 10 pCi/ml for Na-22. The absorber is cooled by the LCW system, which is not a closed loop; therefore the water used to cool down the absorber is considered as surface water. Nevertheless, estimates of the activation of the cooling water are performed using the flux of hadrons with energy higher than 30 MeV in the cooling water lines. This is above the 25 MeV beam energy of PIP2IT, therefore activation of the absorber cooling water is likely to be insignificant.

19 Air Activation

MARS predicted an Ar-41 production rate in the volume surrounding the absorber cone of $4.32 \cdot 10^{-8}$ atoms/proton with about 10% error. Considering a beam intensity of $1.375 \cdot 10^{14}$ proton/sec, with about $2 \cdot 10^7$ sec (63%) of operation in a year, an enclosure volume of $499,000$ cf and an air exchange rate of 1 enclosure volume per hour, the annual release of Ar-41 has been calculated at 0.17 Ci/yr. The activity released is insignificant compared to the lab's total annual release of about 200 Curies. The dose rate due to this air activity is 2 micro-rem/hr, which is insignificant. No action is needed on the part of the experiment to mitigate this level of air activation.

20 Skyshine

The main contributor to skyshine is the neutron dose on the roof of the building (above the enclosure shielding). Gamma skyshine will be much less, because of the photon attenuation length in air compared to that for neutrons. Conservatively, we assumed (1) PIP2IT operates $2 \cdot 10^7$ seconds per year, (2) all of the dose at the roof is due to neutrons, (3) the neutron energy at the roof is 25 MeV. The calculated annual dose due to skyshine is given in Figure 43.

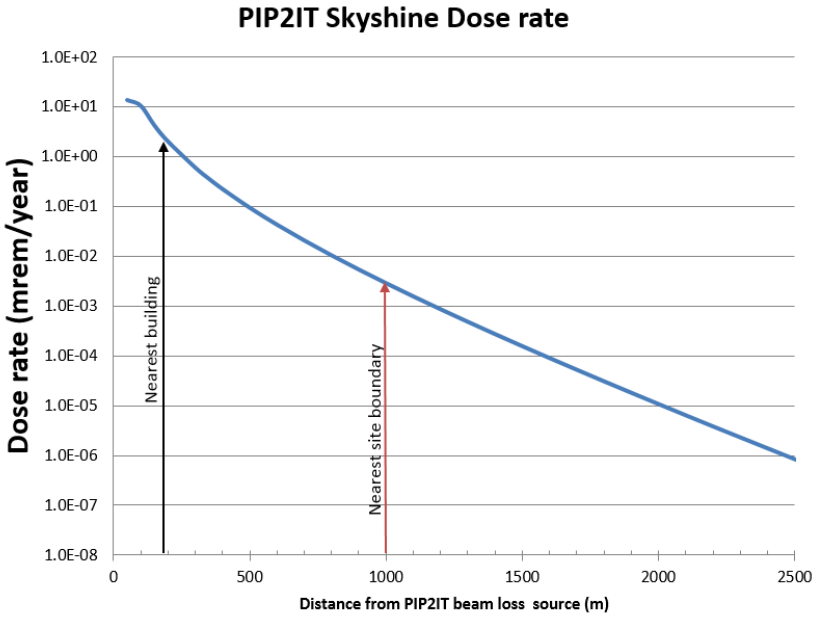

Figure 43: Skyshine from PIP2IT under normal operation.

The skyshine annual doses are marked on Figure 43 for two important locations: The nearest onsite location to PIP2IT facility that may be occupied by members of the public is the Training Center at about 200 m. Note the annual dose at this location is 2 mrem/yr. However, this building is only occupied about 2000 hours in a year, not $2 \cdot 10^7$ seconds (5911 hours). Scaling down the above dose, annual dose at this location is 0.7 mrem. This is much less that the annual dose allowed for the members of public. The nearest site boundary location is about 1000 m from the PIP2IT facility. The annual dose to the members of public at this location is about 3 micro-rems. This is a very insignificant dose, 0.003% of the annual dose allowed to the members of public offsite, from all Fermilab operations.

21 Hydrogen gas evolution from the cooling system

Energy deposition in water above the ionization energy of water molecules breaks the molecule into H and OH radicals. Not all of these recombine; some hydrogen atoms combine with other hydrogen atoms and form H2 gas. The release of this hydrogen gas into the air may form an explosive mixture if the concentration is above 4%. The rate

of hydrogen production can be estimated using calculations from MARS of the energy deposition in the cooling water. The absorber cone has two cooling channels: Channel 1 at the cone nose with a volume of $9.7539 \cdot 10^{-1}$ cm^3, and Channel 2 around the body of the cone with a volume of $1.2024 \cdot 10^2$ cm^3. MARS predicted an energy deposition in Channel 1 of $8.5 \cdot 10^{-9}$ GeV/g/p and an energy deposition in Channel 2 of $1.646 \cdot 10^{-9}$ GeV/g/p. Based on this information and assuming $2 \cdot 10^7$ seconds of beam operation a year, the rate of hydrogen gas production has been calculated to be 42 cc of hydrogen, at STP, in a year. This is a very small amount and therefore we will not have an explosion problem.

22 Field Emission Radiation from HWR and SSR

Eight HWR cavities are expected to operate in the HWR cryomodule at a peak electric field E_{peak} increasing from about $E_{peak} =\sim 4$ MV/m for the first HWR cavity to $E_{peak} =\sim 25$ MV/m for the eighth HWR cavity. RF Tests performed at Argonne National Lab on all eight HWR cavities and reported in [9] indicate that no X-rays have been observed during conditioning of the HWR cavities up to $E_{peak} =\sim 70$ MV/m. As a consequence we do not consider field emission from HWR cavities to be an issue.

Eight SSR cavities are expected to operate in the SSR cryomodule at a peak electric field E_{peak} increasing from about $E_{peak} =\sim 11$ MV/m for the first SSR cavity to $E_{peak} =\sim 23$ MV/m for the eighth SSR cavity. RF Tests performed at Fermilab an reported in [10] on all eight SSR cavities indicate that no X-rays have been observed in 3 SSR cavities and X-rays radiation levels below 4 mrem/hr have been measured for each one of the remaining 5 SSR cavities operating at $E_{peak} =\sim 38$ MV/m. Based on these results, we could expect about 20 mrem/hr from the SSR cryomodule. Attenuation factor of X-rays radiation in air is proportional to $1/d^2$, with d being the distance in ft from the source. If we consider the X-rays from the SSR cavities to generate on axis and if we consider 12 ft as the closest cave outside point (6 ft from the beam axis to the 6-ft East Wall in the inside of the enclosure, from 4) then at the outside of the cave the X-rays radiation is expected to be lower than 0.25 mrem/hr, taking into account only air attenuation of X-rays radiation. As a consequence we do not consider field emission from SSR cavities to be an issue.

23 Summary

The shielding for the PIP2IT enclosure has been analyzed under both normal and accident conditions. The analyses performed for prompt effective dose rates under normal operation at 550 W at the absorber and 10 W at Slit1 are all within FRCM requirements, as reported in respectively Tables 6 and 7. The analyses performed for skyshine, hydrogen gas evolution, and air activation are also all within FRCM requirements. Residual activation near the absorber has also been predicted and dose to personnel in the area will be kept As Low As Reasonably Achievable (ALARA) via standard radiological work controls, such as ALARA plans and Radiological Work Permits. Analyses for ground and surface water activation and muons were not performed since the beam energy is below their production thresholds.

The CMTF building which hosts the PIP2IT enclosure is a Controlled Area. The PIP2IT enclosure will be interlocked to the Radiation Safety Interlock System (RSIS). This system is routinely tested and certified to turn off the critical device(s) for the beamline within one second of detecting an out-of-range or absent input signal. Interlocked detectors will be installed at the South Emergency Exit Labyrinth gate and on the roof of the enclosure. Specific locations and trip levels of radiation detectors interlocked to the RSIS are set by the assigned Radiation Safety Officer (RSO) to ensure compliance with the Fermilab Radiological Control Manual; however, we suggest the trip level on the interlocked detector at the South Emergency Exit Labyrinth gate to be set no higher than 5 mrem in 1 hour so that, for an accident condition occurring anywhere from the exit of the HWR (10 MeV) to the entrance of the absorber (25 MeV), this detector will turn off the injector and limit doses at all locations to within FRCM guidelines. Accidental beam losses below 10 MeV result in dose rates far below FRCM limits. Therefore, the facility can be operated safely at the specified beam parameters.

	FRCM Limit	Dose from Absorber at Normal Operation at **550 W**	
		From Eq. 1 to Eq. 9 (1.5 ft concrete +1 in steel at absorber)	From MARS
	[mrem/hr]	[mrem/hr]	[mrem/hr]
South EE labyrinth	5	1.4	1.1
South EE Labyrinth Short-Circuit-1	5	$5.1 \cdot 10^{-2}$	–
South EE Labyrinth Short-Circuit-2	0.25	$4 \cdot 10^{-2}$	–
South-East Cryo	0.25	$2.1 \cdot 10^{-4}$	$4.3 \cdot 10^{-3}$
South-East Cryo Short-Circuit	0.25	$1.5 \cdot 10^{-3}$	–
Cryo Penetration	0.25	$1 \cdot 10^{-3}$	–
Penetration Block Section	0.25	$4 \cdot 10^{-6}$	–
North Low Energy Labyrinth	0.25	$1.3 \cdot 10^{-4}$	–
Roof	5	0.4	1.2
Walls 6 ft	0.25	$1.2 \cdot 10^{-4}$	–
Walls 3 ft	0.25	$2 \cdot 10^{-2}$	–

Table 6: Maximum Dose at different location of the enclosure from the absorber under normal operation at 550 W.

	FRCM Limit	Dose from Slit1 at Normal Operation at **10 W**	
		From Eq. 1 to Eq. 9 (No Shielding at Slit1)	From MARS
	[mrem/hr]	[mrem/hr]	[mrem/hr]
South EE labyrinth	5	1.4	1.3
South EE Labyrinth Short-Circuit-1	5	$4.9 \cdot 10^{-2}$	–
South EE Labyrinth Short-Circuit-2	0.25	$1.6 \cdot 10^{-3}$	–
South-East Cryo	0.25	$7.8 \cdot 10^{-3}$	$9.8 \cdot 10^{-2}$
South-East Cryo Short-Circuit	0.25	$5.4 \cdot 10^{-2}$	–
Roof	5	1.2	1.6
Walls 6 ft	0.25	$3.6 \cdot 10^{-4}$	–
Walls 3 ft	0.25	$1.6 \cdot 10^{-2}$	–

Table 7: Maximum Dose at different location of the enclosure from HEBT Slit1 under normal operation at 10 W.

24 Acknowledgment

The author would like to thank J. Anderson, W. Higgins, W. Schmitt, K. Vaziri and M. Vincent for many discussions and careful reading of this document, P. Kasper for discussion on the HINS Linac Shielding Assessment, C. Baffe, L. Prost and S. Shemyakin for their help in shielding the absorber, S. Wesseln for the drawings of the absorber and N. Mokhov and his group for help with the code MARS.

References

[1] Fermilab Radiological Control Manual,
http://eshq.fnal.gov/manuals/frcm.

[2] Fermilab Grid Computing
https://www.fnal.gov/pub/science/computing/grid.html

[3] A. H. Sullivan, A Guide to Radiation and Radioactivity Levels near High Energy Particle Accelerators, 1992

[4] P. Kasper, The HINS Linac Shielding Assessment, FNAL document, January 27, 2011.

[5] J. Cossairt, Radiation Physics for Personnel and Environmental Protection, Fermilab TM-1834, 201120161.

[6] Fermilab TM-2470, MARS Star Density Results for Shielding Applications.

[7] N.V. Mokhov and C.C. James, "The Mars Code System User's Guide, Version 15 (2016)", Fermilab-FN-1058-APC (2017),
https://mars.fnal.gov/

[8] A. Leveling, PXIE Preliminary Shielding Assessment, Project X Document 1051-v2, June 13, 2012.

[9] P. Ostroumov, Development of Low-Beta Superconducting Cavities for Large Accelerators, Slide 9, IPAC-18, April 29 - May 4, Vancouver BD, Canada.

[10] A. Sukhanov, Characterization of SSR1 cavities for PIP-II linac , Proceedings of SRF 19, Dresden.

[11] A. B. Chilton, J. K. Shultis and R. E. Faw, Principles of Radiation Shielding, Prentice-Hall, Inc., New-Jersey, 1984.